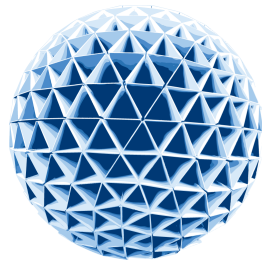


# Transverse Stress of ReBCO High-Temperature Superconductors for Future Compact Fusion Reactors



UNIVERSITY  
COLLEGE  
TWENTE

**Katrīna Rimša**

Capstone Project

BSc Technology, Liberal Arts & Sciences

University College Twente

Enschede, The Netherlands

June 20, 2024

Supervisors:

**Dr. ir. Anna Kario**

**Dr. ir. Simon Otten**

**Dr. José Alfredo Álvarez-Chávez**

## Abstract

With increasing concern about climate change, demand for a sustainable electrical energy has skyrocketed. Green, reliable, and efficient energy sources are needed to facilitate this rising demand. To meet these requirements, a nuclear fusion power plant ITER is being built in the south of France. Besides ITER, future fusion compact reactor is a prospective energy production source, that would utilise high-temperature superconductors. These superconductors are essential to producing 20 T strong magnetic fields for achieving plasma confinement in the compact fusion reactor. Due to the high magnetic field, the superconductors would be subject to high electromechanical forces. Different Lorentz force component limitations of the state-of-the-art ReBCO tape need to be studied to prevent tape damage. One of the components is the transverse stress.

Critical current against transverse stress measurements can be carried out using a transverse press in cryogenic conditions. Two press setups were explored. Bennie press was found to be improper for critical current against transverse stress measurements for the state-of-the-art ReBCO tape. A Rintje Ritsma transverse stress press setup was proposed, which was designed to improve the limitations of the Bennie press. One of the findings showed no transverse stress resistance. However, after improving the Rintje Ritsma press setup, critical current degradation did not occur until 240 MPa high transverse stress, with irreversible critical current occurring after 490 MPa. The Rintje Ritsma press setup must be further improved to validate the results.

## **Acknowledgements**

This Capstone Project becomes a reality with the kind support of many individuals. I would like to extend my sincere thanks to all of them.

Most importantly, thanks to Dr. ir. Anna Kario, Dr. ir. Simon Otten and Dr. José Alfredo Álvarez-Chávez for their continuous guidance, invaluable knowledge, and motivation over the last four months. Thank you to Sander Wessel for the creative design ideas and teaching me how to work with the highly advanced workshop equipment. I wish to thank Ruben Lubkemann for introducing me to the Bennie press and standing by my side while I was executing my first critical current measurement. Moreover, I would also like to thank Lennard Rietkerk for his assistance in applying 69 kN force to my sample, kindly sharing the monitor at the office, and, most notably, for believing in me. Thanks to the TCO for their speedy production process. Without you, this project would not have been finished on time. Finally, I would like to extend my deepest appreciation to my family, friends, and UCT community for their consistent support and motivation.

# Contents

<b>Introduction to ReBCO High-Temperature Superconductors for Future Compact Fusion Reactors</b>	<b>5</b>
<b>Understanding the Core: The Theory Behind Transverse Stress of ReBCO High-Temperature Superconductors for Compact Fusion Reactors</b>	<b>7</b>
Superconductors . . . . .	7
Compact Fusion Reactors . . . . .	8
High-Temperature Superconductors . . . . .	8
State-of-the-Art ReBCO Tape . . . . .	8
Transverse Stress of ReBCO Tape . . . . .	9
<b>Methodology of Transverse Stress Experiments on ReBCO tape</b>	<b>11</b>
Bennie Press . . . . .	11
Bennie Press Homogeneity Examination at Room Temperature . . . . .	12
Bennie Press Homogeneity and Gradual Unloading Failure Improvement at Room Temperature . . . . .	12
Designing the Rintje Ritsma Press . . . . .	14
Critical Current Against Transverse Stress at 77 K Measurements . . . . .	14
<b>Results and Data Analysis of Bennie Press Homogeneity, Rintje Ritsma Press Design and Critical Current Against Transverse Stress</b>	<b>17</b>
Bennie Press Homogeneity at Room Temperature . . . . .	17
Rintje Ritsma Press Design . . . . .	19
Critical Current Against Transverse Stress for Sample #1 . . . . .	22
Critical Current Against Transverse Stress for Sample #2 . . . . .	24
Critical Current Against Transverse Stress Result Comparison Between Sample #1 and Sample #2 . . . . .	27
<b>Outlook</b>	<b>29</b>
Limitations of the Bennie Press Homogeneity Examination . . . . .	29
Limitations of the Rintje Ritsma Press Design . . . . .	29
Implications for Future Research with the Rintje Ritsma Press . . . . .	30
Contextual Exploration . . . . .	31
<b>Conclusion</b>	<b>33</b>
<b>Appendix</b>	<b>40</b>
Technical Drawings for the Rintje Ritsma Press Assembly Items . . . . .	40

# Introduction to ReBCO High-Temperature Superconductors for Future Compact Fusion Reactors

With the rising alert for climate change, severe actions are required to limit the production of greenhouse gases [1]. Transitioning to electrical energy to power our homes and transport increases the demand for more energy generation worldwide [2]. Focusing on greener energy sources rather than burning more fossil fuels is crucial to restrain carbon emissions and facilitate the increase in energy demand. In addition, more energy-efficient electricity transmission materials should be investigated because around 8% of the generated electricity is lost in the transmission power lines due to Joule heating [3][2].

Superconductors exhibit no electrical resistance when cooled down below a specific temperature, called the critical temperature [4]. With no resistance, superconductors do not generate any heat, making it possible to transmit electricity without any losses in the direct current power lines [5]. Moreover, superconductors can carry larger currents and, thus, magnetic fields throughout the same wire cross-section compared to copper or aluminium [6]. Due to these advantages, superconductors are used in magnetic resonance imaging (MRI), particle accelerators, and experimental fusion devices [7].

Superconductors can be classified based on their critical temperature. Low-temperature superconductors (LTS) are used in current superconductor applications and the world's largest fusion reactor ITER [8]. To achieve superconductivity in LTS, liquid helium with a boiling temperature of around 4.2K is required [9]. The coolant is expensive, and helium resources are limited [10]. While the ITER design was in development, fusion research companies developed a new technology concept – a compact fusion reactor (CFR) [11]. These compact reactors need magnetic fields of 20 T, which is a relatively high magnetic field compared to the ITER (13 T) [12][13]. The CFR would employ high-temperature superconductors (HTS), which exhibit superconductivity at temperatures above 4.2 K and enable stronger magnetic fields essential for successful plasma confinement [7]. Even though the HTS material is still costly, other expenses associated with building and maintaining future compact reactors are significantly lower than those associated with conventional large reactors because of their smaller size [14]. Moreover, due to the private sector's interest in this technology, the research process is more dynamic in contrast to the conventional large fusion reactors, where the majority of funds come from the governments or European Union budget [15][16]. CFR can also allow for more decentralised energy generation by placing it in various areas in a country [17]. However, the high HTS costs and physical properties, among mechanical limitations, are still relevant factors delaying the development of the technology [7].

Rare-earth barium copper oxide (ReBCO) is a high-temperature superconductor that is currently the only realistic option for use in compact fusion reactors [18]. Only using ReBCO, the magnetic field magnitude of 20 T can be realised in an energy-efficient way [7]. However, there are challenges with the ReBCO material. Due to the physics of the superconductivity of ReBCO, it can only be manufactured as a tape (coated conductor). In the magnet of 20 T, these tapes will be subject to a high Lorentz force. When the mechanical strength limit is achieved, ReBCO's irreversible strain limit is exceeded, which permanently degrades the critical current and leads to the loss of superconductivity [19]. Identification of the tape mechanical strength limit is useful for coil pre-stressing, which is a prevention against tape delamination. The Energy, Materials & Systems (EMS) research

group at the University of Twente works closely with tape manufacturing companies (Faraday Factory Japan and Shanghai Superconductor Technology) and research organisations, such as the European Organization for Nuclear Research (CERN). A previous study at EMS shows that ReBCO tape has a transverse stress limit at 560 MPa [19]. ReBCO tape with a 40  $\mu\text{m}$  copper thickness was transversely pressed using the Bennie press at 77 K. However, the state-of-the-art ReBCO tape has changed the copper (Cu), substrate, and ReBCO layer thickness, impacting tape's transverse limits. EMS performed experiments on the state-of-the-art ReBCO as well. However, the results were non-reproducible, and there is suspicion about an inhomogeneous pressure distribution in the Bennie press [20]. EMS must verify the estimated change in the transverse stress limitation to present the data set of how large the different Lorentz force components' (tensile, shear, transverse) limits are to the collaborating laboratories for the state-of-the-art ReBCO. Moreover, it is a verification for the manufacturing companies of their product's mechanical specification. In this research, the limitations of the state-of-the-art ReBCO tape transverse stress component will be investigated. Thus, the main research objective is to:

***Examine one of the mechanical load components—the transverse stress limitation of state-of-the-art ReBCO tape in relation to the degradation of the critical current.***

To achieve the main objective, two sub-objectives are defined:

1. *Validating Bennie press suitability for critical current against transverse stress measurements for the state-of-the-art ReBCO tape with respect to homogeneous pressure distribution;*
2. *If the Bennie press is concluded to be unsuitable, propose a new transverse press design applicable to the state-of-the-art ReBCO critical current against transverse press measurements.*

The primary aim of the research is to analyse the ReBCO coated conductor provided by the manufacturing company. The study will focus on measuring and limitations related to critical current degradation in state-of-the-art ReBCO tape with a 5  $\mu\text{m}$  thin copper layer.

# Understanding the Core: The Theory Behind Transverse Stress of ReBCO High-Temperature Superconductors for Compact Fusion Reactors

## Superconductors

### Superconductors

Superconductor is a material whose electrical resistance goes to zero under the critical temperature [21]. If a material does not have electrical resistance, it can carry current unimpeded by any obstructive forces and requires minimal or no external voltage [22]. However, there is only a certain amount of current, called the critical current, that a material is able to achieve without losing its superconductivity. Above the critical current, the superconductor develops resistance [23]. Moreover, currents generate magnetic fields. The magnitude of a magnetic field in a certain coil geometry bore is proportional to the current density in the windings [24]. That is why superconductors produce higher magnetic fields while consuming reasonable amounts of energy compared to conductors [25]. There is a constraint on the magnitude of the magnetic field under which the material is superconducting, which is called the critical field. If the critical field is exceeded, material loses its superconductivity [26]. Overall, there are three main superconducting properties - critical temperature, critical current, and critical field. Relationship between these properties is visualised in a plot called critical surface, which is unique for every superconductor. In Figure 1, critical surface of  $Nb_3Sn$  and  $NbTi$  is depicted.

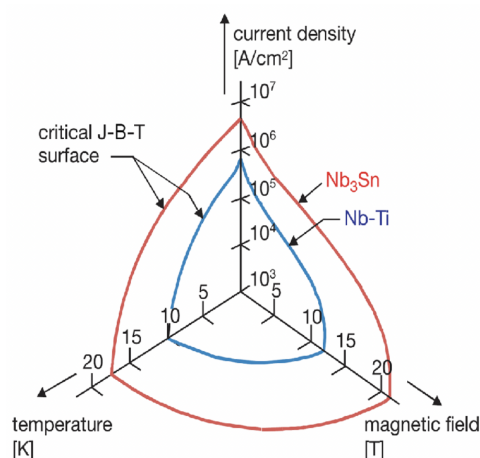


Figure 1: Critical surface of  $Nb_3Sn$  vs  $NbTi$  [27].

There is another essential superconductor property - the mechanical strength, above which the material's electromagnetic strain limits are exceeded and the critical current drops [28]. This happens because the critical current is reversibly or irreversibly changed below the mechanical strength value [29]. Due to the anisotropic nature of the ReBCO superconductor, the mechanical strength limit varies in different directions [30]. The relationship between one of the mechanical strength's components, the transverse stress, and the critical current will be further investigated in this report.

## Compact Fusion Reactors

Compact fusion reactors might be the key technology to accelerate the development of fusion energy worldwide [31]. CFR are fusion devices reduced in size and power output compared to current research fusion reactors. The CFR could be up to 10 times smaller in volume while producing only about 5 times less power output than the ITER. Due to the significantly reduced dimensions, the CFR design needs stronger magnetic fields to facilitate the aspect ratio [14]. The aspect ratio is the proportionality of the major over minor radius of the tokamak [32]. A lower aspect ratio increases plasma stability limits. A minimal aspect ratio can be achieved in a spherical tokamak, which is the primary tokamak design considered for the CFR [33]. However, a low aspect ratio also means that more powerful magnetic fields need to be generated to confine the plasma and keep it away from the chamber walls [34]. To achieve plasma confinement in the compact reactor, superconducting magnets that can create 20 T strong magnetic fields are required [35]. Currently, only HTS can satisfy this requirement in an energy-efficient way [7].

## High-Temperature Superconductors

High-temperature superconductors are materials that exhibit no electrical resistance at relatively high temperatures compared to low-temperature superconductors (LTS). While the LTS exhibit superconductivity at around absolute zero temperature and require liquid helium as a coolant, some HTS exhibit zero resistivity up to 92 K [36]. In a CFR, the superconductor would be cooled down to 20 K to optimize all critical surface properties. Compared to LTS, where cooling must be done to around 4-5 K with helium, cooling HTS magnets to 20 K with, for instance, cryocoolers is considerably cheaper [37][10]. More importantly, HTS has a higher current density than LTS at fields above 20 T [38]. The critical current begins to decrease rapidly for Nb<sub>3</sub>Sn after 11 T already, but ReBCO can double the field because of its 100 times higher current density in the 22 T coil field [14]. These properties make HTS especially attractive for compact fusion development. The main class of high-temperature superconductors is a copper-oxide combination with rare-earth barium. The critical temperature of ReBCO is 92 K, making it suitable for applications in LN<sub>2</sub> [39]. Since the critical current, field, and load depend on each other, the property values differ per application and product specifications. For instance, at the required magnetic field for CFR operation of 20 T, ReBCO can exhibit up to 1200 MA/m<sup>2</sup> critical current density in a coil with a superconductor fraction of 7% [14]. Moreover, at 370-440 MPa transverse stress, the ReBCO magnet can still operate in a superconductive state [40]. Meanwhile, Nb<sub>3</sub>Sn would have an upper critical field of 20T with a maximum transverse load of 200 MPa exerted on the cable [41]. These values were obtained at 4.2 K. Overall, due to ReBCO's high current density and mechanical strength, it is the most auspicious type of high-temperature superconductor to accelerate fusion development [7][29].

## State-of-the-Art ReBCO Tape

ReBCO coated conductor, the promising material for compact fusion reactor magnets, exhibits exceptional physical properties, enabling high current-carrying capacity and mechanical strengths [29]. However, it comes with its challenges. While other superconductors are produced in a wire shape, ReBCO's sensitive atomic structure requires flat tape-shape manufacturing [14]. ReBCO's atomic structure is sensitive to the crystallographic



orientation [42]. Small grain boundary misorientation angles can jeopardise the desired current flow [29]. Thus, the fabrication process of a long tape is costly compared to other conductors. High cost is a considerable barrier to large-scale application of the tape conductor [43].

The ReBCO coated conductor can be manufactured in 0.1 - 0.2 mm thickness, 4 - 12 mm width and consists of six layers (Figure 2). Coated conductor and layers might differ per manufacturer due to variations in production techniques. Thus, most of the presented tape design specifications are in range format.

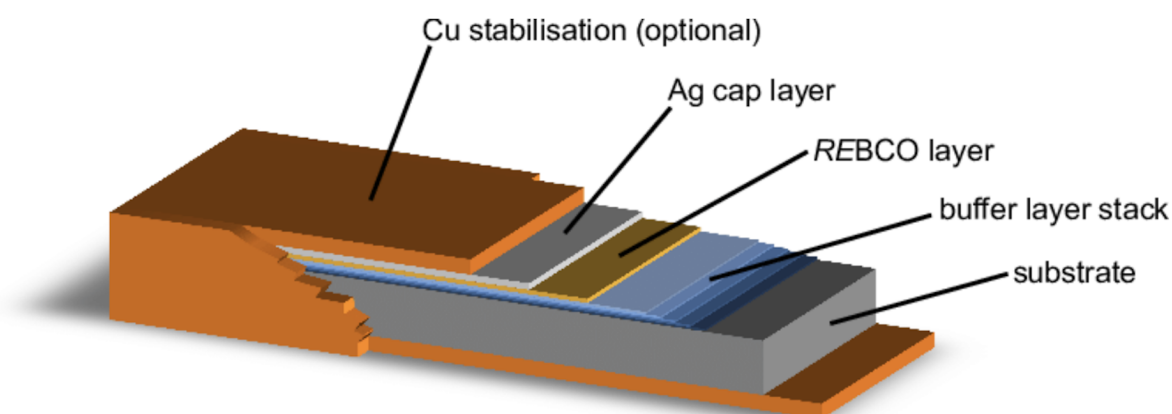


Figure 2: Schematic layout of ReBCO tape layers [44]. Layers may differ per manufacturer.

Copper (Cu) coating layers can vary from 4 to 100  $\mu\text{m}$  per side and act as stabilisers [45]. State-of-the-art ReBCO tape has a 5  $\mu\text{m}$  thin Cu layer. Decreasing thickness of Cu layer has been shown to increase the transverse stress limitation of the coated conductor [19][46]. The Cu layers limit possible quench<sup>1</sup> phenomena and provide a parallel current path [48][46]. The silver (Ag) layer (1-24  $\mu\text{m}$ ) connects ReBCO with Cu coating and serves as a protective layer of ReBCO. It manages the oxygen diffusion for the ReBCO, which is essential for the superconductor's functionality [49] [50]. ReBCO layer (1.5-5  $\mu\text{m}$ ) carries the superconducting current and the oxide buffer layers (0.07-2  $\mu\text{m}$ ) avoid metal pollution from substrate into the ReBCO layer and also functions as an oxygen diffusion barrier. Moreover, it is an adhesive between substrate and ReBCO, which is necessary because of the differences in crystal structures between the two layers [51]. The buffer layer provides texture for grain alignment [52]. The substrate layer (20-100  $\mu\text{m}$ ) is preferably made out of a Hastelloy and provides the overall strength of the tape. It is one of the main reasons behind the conductor's mechanical strength [53]. Overall, the coated conductor exhibits an outstanding ability to carry large current densities due to the almost perfect crystallographic orientation between the layers [54]. However, delamination is a major challenge for the multi-layered conductor that is discussed in more detail in the following section.

## Transverse Stress of ReBCO Tape

For ReBCO coated conductor to be used in a compact tokamak type fusion reactor, it must first be assembled into a d-shaped toroidal field coil magnet (Figure 3). The 20 T high magnetic field inside the reactor induces strong electromechanical forces on the outside of the coil, in-between the tapes and even its layers. For example, [56]

<sup>1</sup>An unexpected and rapid loss of superconductivity and return to normal state. As result, material heats up quickly, possibly causing damage if not controlled adequately [47].

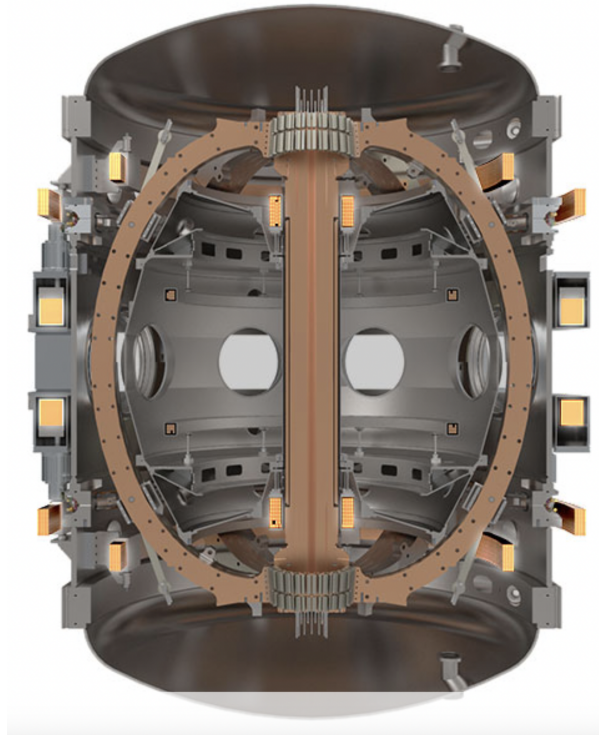


Figure 3: Two d-shaped HTS magnet coils inside a ST40 compact fusion reactor with a major radius of 0.4 m [55].

measured 382 kN/m at 11 T magnetic field using the HTS tape. This value is equal to the unit force value of seven Boeing 747-8f aircrafts stacked on each other. However, more important is to emphasise the different components of this force. The direction of the Lorentz force depends on the direction of the magnetic field which varies for different coils [57]. In combination with the anisotropic atomic structure of the tape, the material's superconducting properties can significantly vary with the direction of the magnetic field [58]. For instance, a solenoid coil faces hoop stresses caused by the electromechanical force, which has tensile, shear and transverse stress components acting on the conductor [29]. It can lead to several issues within the coated conductor affecting its superconductivity, such as irreversible degradation of critical characteristics, brittle layer fracture and delamination [59]. Delamination occurs when the adhesive buffer layer detaches from the ReBCO layer, which significantly degrades the performance of the tape [60]. Fortunately, delamination could potentially be managed by pre-stressing the coil [61]. To avoid damaging the coil during the treatment, mechanical limitations of the Lorentz force components, including the transverse stress, of the ReBCO tape must be investigated.

# Methodology of Transverse Stress Experiments on ReBCO tape

## Bennie Press

The Energy, Materials and Systems (EMS) research group at the University of Twente has previous experience with mechanical testing of LTS ( $\text{Nb}_3\text{Sn}$ ) and HTS (ReBCO and Bi-2223) samples with Bennie press. The press was designed for transverse stress measurements at 4.2 K with an external magnetic field, which meant that the press has a peculiar design made to fit in a small magnet. The maximum transverse force of the Bennie press is 6kN and it was purposed for  $\text{Nb}_3\text{Sn}$  and Bi-2223 transverse testing up to 300 MPa [62].

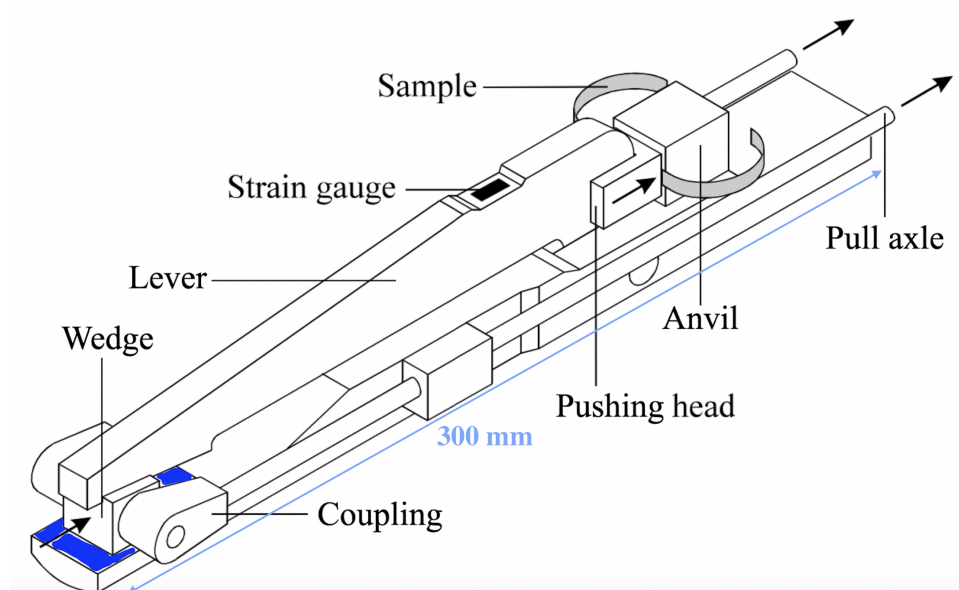


Figure 4: Bennie Press [62].

According to [62], the stainless steel wedge and the titanium pushing head are the main contributors to the homogeneous pressure application on the sample. When force is applied, the pull axle and coupling displace the wedge in the direction of the arrows on the sliding area (indicated in blue in Figure 4) and the pushing head can then make direct surface contact with the sample. The pull axle is connected to a turning knob, which is rotated by hand. The lever acts as a force transfer between the wedge and the pushing head. It also has a strain gauge, which is crucial for pressure calibration and is used for force measurement. The pushing head has curved design components on both sides that ensure aligned force application.

However, by using Bennie press for transverse testing of the ReBCO tape, the obtained results were non-reproducible [20]. Additionally, unloading mechanism was malfunctioning above pressures of 300 MPa. The unloading is supposed to be gradual, but above 300 MPa, the force could only be released at once. Thus, press suitability must be validated before the results of the ReBCO transverse stress experiments can be considered legitimate. The first step was to study the homogeneity of pressure distribution on the ReBCO tape in the Bennie press at room temperature. The following sections also present how the homogeneity and faulty unloading mechanism were attempted to be later improved and resolved, respectively.

## Bennie Press Homogeneity Examination at Room Temperature

The state of pressure distribution homogeneity was explored using the Fujifilm pre-scale due to its convenient application and availability at the Superconductivity Laboratory. Fujifilm pre-scale is a single use, pressure sensitive film [63]. Overall, there are nine different films available based on the pressure ranges depicted in Figure 5. In this experiment, only film types highlighted with red frame were used because of the relevant pressure ranges of Bennie press.

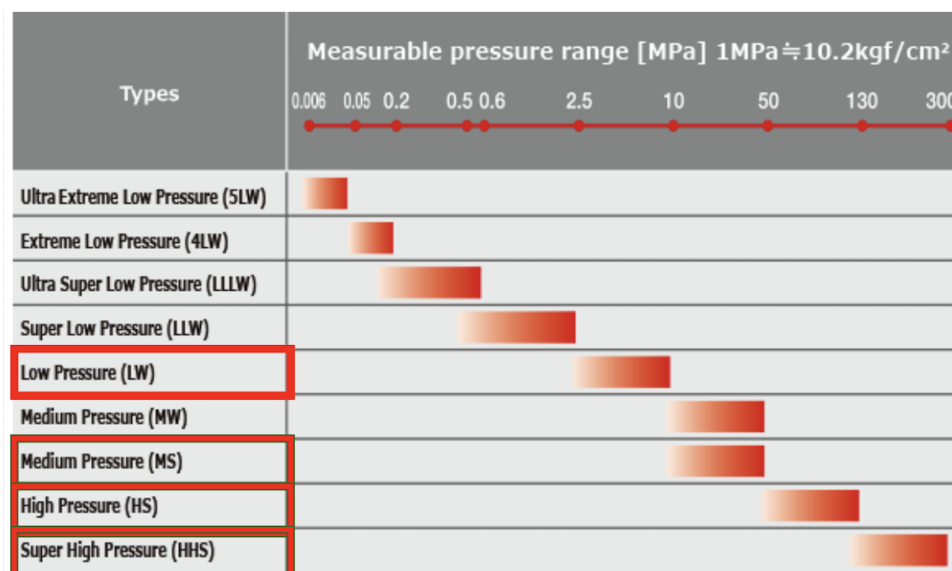


Figure 5: Pressure ranges for different film types [63].

Each film was cut around 30x30 mm and placed in-between the sample and the pushing head. The corresponding film maximum pressure value was applied. For example, for the LW film, 10 MPa pressure was applied. Then, the pressure was released to 0 MPa and LW film was replaced by the MS type. Then, 50 MPa was applied and released. The remaining HS and HHS films were examined following the same steps. For more accurate results, minimum and middle pressure values for some films were also examined.

To determine the applied pressure value, strain gauge calibration results were used. Calibration was previously done by the EMS, from which they obtained the force-resistance linear dependence. The force values were divided by the pushing head area to obtain the stress value in MPa. The formula was applied to the resistance values displayed on a KEITHLEY 2700 multimeter connected to the linear stainless steel strain gauge on the lever.

## Bennie Press Homogeneity and Gradual Unloading Failure Improvement at Room Temperature

Since the Bennie press was designed in such a way that the wedge is one of the items accountable for both homogeneous force application and gradual force release, the mechanical state of the wedge was studied. Scratches on the bottom of the wedge (highlighted in blue in Figure 6) and engravings on the sliding area (Figure 7) indicated the possibility of uneven movement of the wedge when loading and unloading. Thus, the stainless steel wedge was replaced with a new bronze wedge. Bronze was the chosen material due to its smaller friction coefficient in

comparison to stainless steel (0.19 and 0.40, respectively [64][65]).

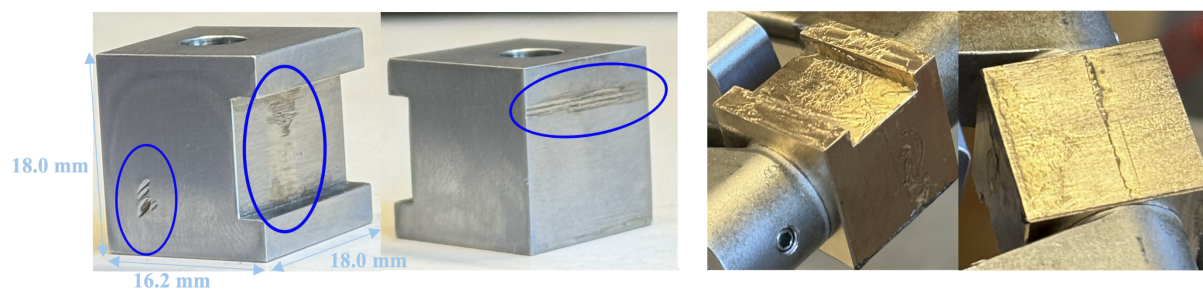


Figure 6: Stainless steel wedge (left) and new bronze wedge (right). Both wedges are equal in dimensions. Bronze wedge was covered in oil lubricant, which was later replaced with graphite.

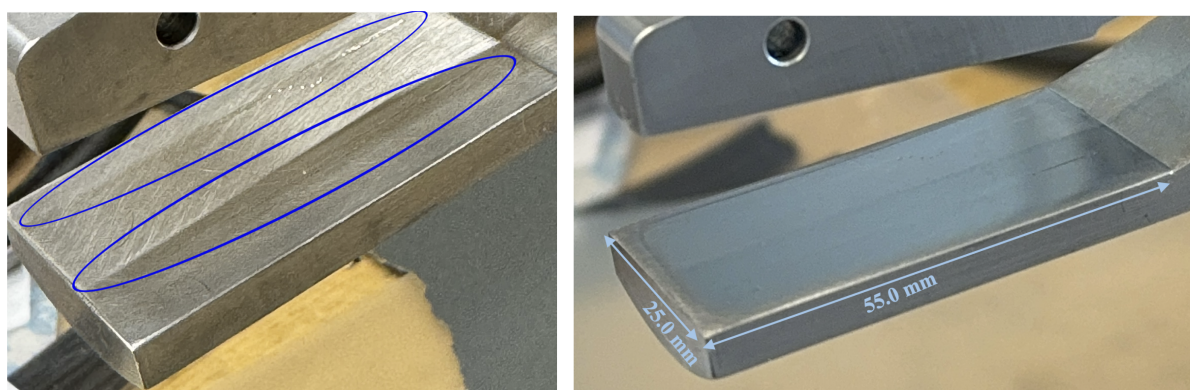


Figure 7: Sliding surface area before (left) and after (right) polishing.

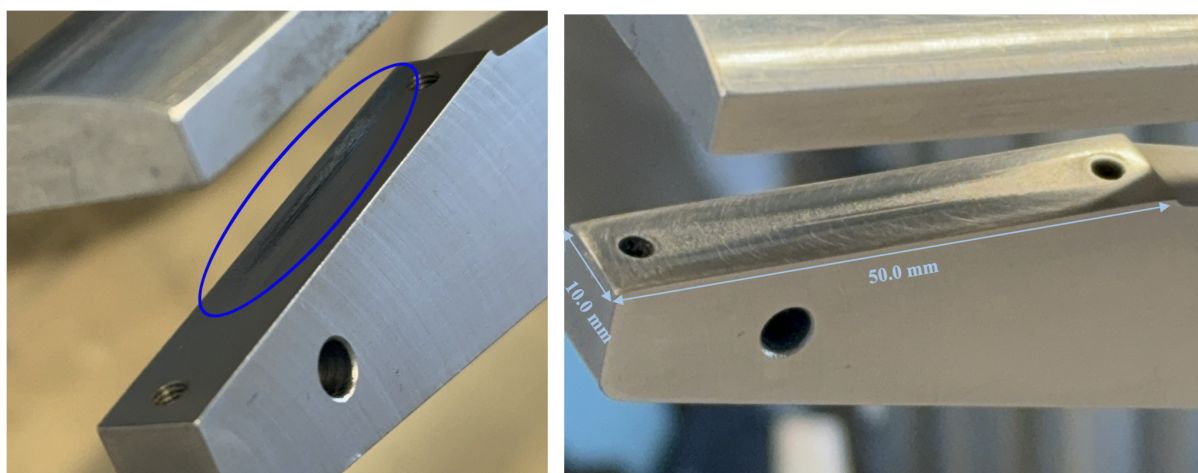


Figure 8: Lever bottom surface area before (left) and after (right) polishing.

Sliding surface and the lever bottom surface, which are in direct contact with the wedge, were polished to remove any engravings and scratches (Figure 7 and 8). Sandpapers with grit numbers of 800, 1000 and 1200 were used. Grit numbers refer to the number of particles that can fit through a square inch filter [64]. Thus, the higher the grit number, the smoother the surface of the material that is being sanded. Additionally, graphite was applied as a lubricant to limit any friction among the press elements. Afterwards, Bennie press homogeneity examination was repeated as described in the section above.

## Designing the Rintje Ritsma Press

The design of the new press setup was based on two factors. Firstly, the limitations of Bennie press were mitigated in the new setup. Secondly, the functionality requirements are dependent on the experimental methodology of the critical current measurements (described further in the chapter). EMS assisted the researcher in the design process by sharing relevant knowledge about the process of critical current against transverse stress measurements at 77 K so all necessary experimental elements and equipment are included in the final design.

Design requirements based on Bennie press limitations (1-2) and requirements for critical current against transverse stress at 77 K measurements, which are not covered by the requirements before (3-8):

1. Homogeneous pressure distribution on the sample;
2. Gradual force release;
3. Sample must be under LN<sub>2</sub> throughout the whole duration of the measurement;
4. Force or strain measuring device;
5. Force alignment in the sample area;
6. Current application;
7. Sample voltage measurement;
8. Quench protection.

The requirements identified above were later adjusted and specified in greater detail based on the availability of the materials and equipment, which will be discussed in the Rintje Ritsma press design results section.

## Critical Current Against Transverse Stress at 77 K Measurements

Critical current against transverse stress measurements at 77 K were carried out using Rintje Ritsma press setup as seen in Figure 13. Preparation and experimentation took two days per sample measurement. One day was spent arranging the setup. Preparation included the installation of the ReBCO sample on the titanium base plate by bolting voltage taps and copper blocks to the plate and pressing them on the tape using indium foil. Then, all electrical equipment was connected to the setup as depicted in Figure 9.

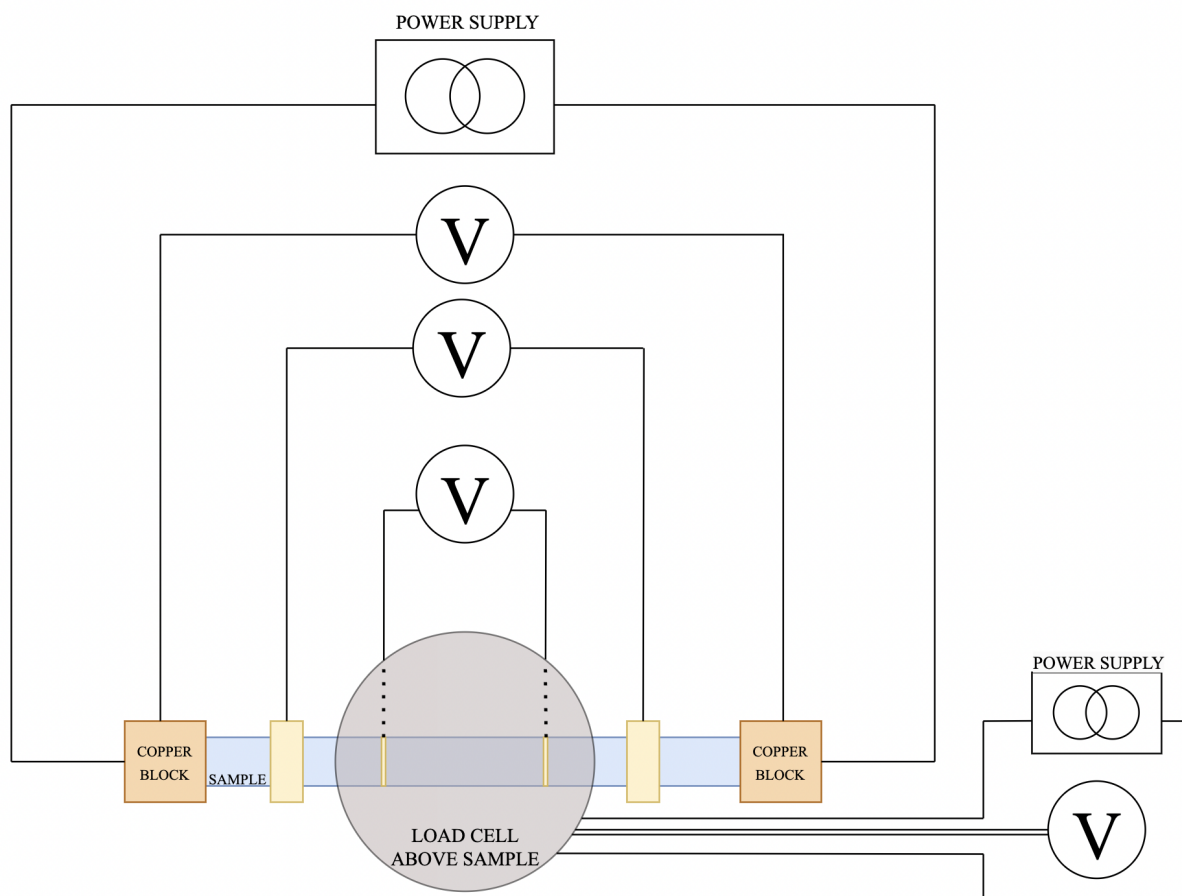


Figure 9: Electrical setup for the critical current against transverse stress measurement for the ReBCO tape.

For the sample #1 measurement, two KEITHLEY 2182A nanovoltmeters were used to measure voltage between two points on each side of the pushing block (73 mm distance) and two copper wires on the copper blocks for quench detection. For the second sample measurement, another pair of voltage taps was added closer to the pushing block (35 mm distance). Thus, a third KEITHLEY 2182A nanovoltmeter was connected to the setup. Two current leads were connecting the SM 15-400 power supply. Power supply elc ALF1501D was used for the load cell 10 V excitation and KEITHLEY 2000 multimeter for load cell voltage readings. Once the electrical equipment was connected, the cryogenic setup was assembled.

Measurements were carried out on the second day. When  $\text{LN}_2$  was poured into the container and the V-I data acquisition program was set up, the critical current at the setup weight (18.62 N weight or 0.16 MPa pressure) was measured. Further in the report, the setup weight will be considered as 0 N. The critical current was determined from the V-I curve. The idea behind a V-I curve is that current is supplied in small steps (n+3 amps, for example) and voltage across the sample is measured for each step. When tape is in the superconducting state at 77 K, it should show little to no voltage when below critical current. When the critical current is exceeded, voltage starts increasing. At a certain voltage value ( $100 \mu\text{V m}^{-1}$  [66]), called the threshold electric field criterion, the critical current was defined and power supply was stopped. Then, 50 MPa pressure was applied and critical current was measured again following the same steps. The transverse load value was determined by the weight gauge on top of the press. The load was divided by the contact area to obtain the exerted transverse stress value. The reversibility

of the current degradation was measured at 0 MPa after the transverse load measurements exceeded the acceptable critical current variation range. Pressure was applied in steps of 10-20 MPa up to 630 MPa. The choice for the maximum pressure range was based on a previous study [19]. 40  $\mu\text{m}$  Cu thickness of the ReBCO tape showed transverse stress limitation at approximately 560 MPa. In this research, a sample with a 5  $\mu\text{m}$  thin Cu layer per side was used. Thus, the expected transverse stress limitation was around 600-700 MPa [19]. The  $\text{LN}_2$  was refilled after every four measurements to prevent warming up the sample.



# Results and Data Analysis of Bennie Press Homogeneity, Rin-tje Ritsma Press Design and Critical Current Against Transverse Stress

## Bennie Press Homogeneity at Room Temperature

Bennie press homogeneity at room temperature was examined in two cases. Firstly, the homogeneity of the press after the critical current measurements done by the EMS (hereinafter referred to as the initial Bennie press homogeneity examination). Secondly, Bennie press homogeneity after attempting to improve it by replacing the stainless steel wedge with a new bronze wedge and polishing the sliding surfaces (hereinafter referred to as the final Bennie press homogeneity examination).

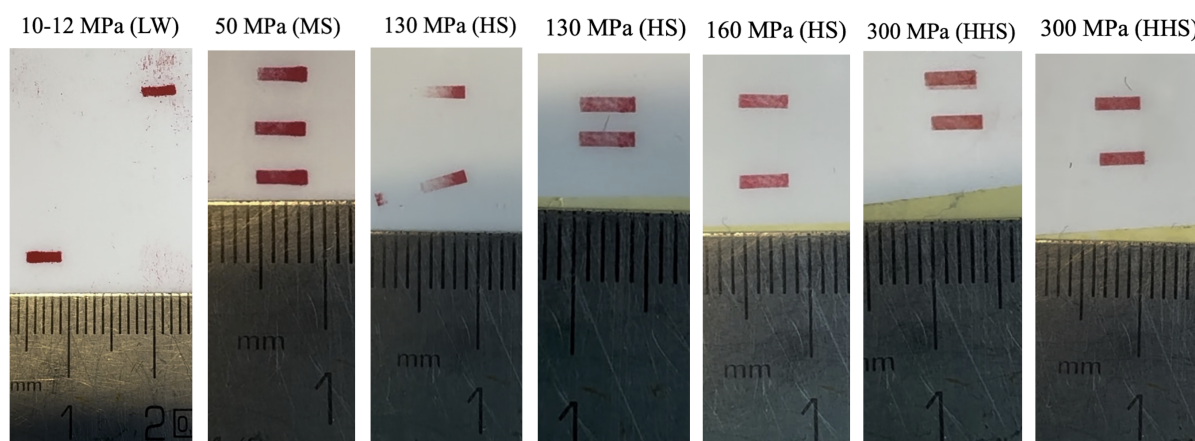


Figure 10: Initial Bennie press homogeneity results.

To validate Bennie press suitability for ReBCO critical current against transverse stress measurement, homogeneous pressure distribution over the sample is required at all pressure ranges at 77 K. Thus, the expected film results at room temperature are best depicted in Figure 10 at 300 MPa. It shows uniform pressure distribution throughout the whole sample area, which faces direct contact with the pushing head. Force application would be considered homogeneous if the uniform pressure distribution was reproduced in all films. From Figure 10, it can be claimed that occasional inhomogeneity is obtained due to the gradient colouring best seen at 50 MPa and 130 MPa. The inhomogeneous pressure distribution means that the sample could have been damaged on the right side earlier than predicted during the critical current measurements, which is in accordance with the results of the critical current against transverse stress measurements at 77 K by using the Bennie press with the state-of-the-art ReBCO tape [20]. The inhomogeneous pressure application might have been caused by the non-gradual wedge movement due to the engravings and scratches visible in Figures 6, 7 and 8. On top of that, considering that the Bennie press was initially designed for smaller stress levels suitable for  $\text{Nb}_3\text{Sn}$ , the pushing head area was reduced to achieve the higher stress limits of ReBCO, which may have contributed to the misalignment.

Moreover, during the film measurements, unloading mechanism failure was observed above 250 MPa. In practice, it meant that gradual force release was difficult because the wedge would get stuck when going downward

on the sliding area. It could be improved by applying external force with hands while turning the knob, which, together with the pull axle, would add even more force on the wedge to move down and release pressure off the sample. However, this approach is not optimal and was mitigated as well.

After polishing the sliding and lever bottom surface was done and bronze wedge was installed, final homogeneity tests were carried out to explore whether any improvements in homogeneity and force unloading could be observed. The results are depicted in Figure 11.

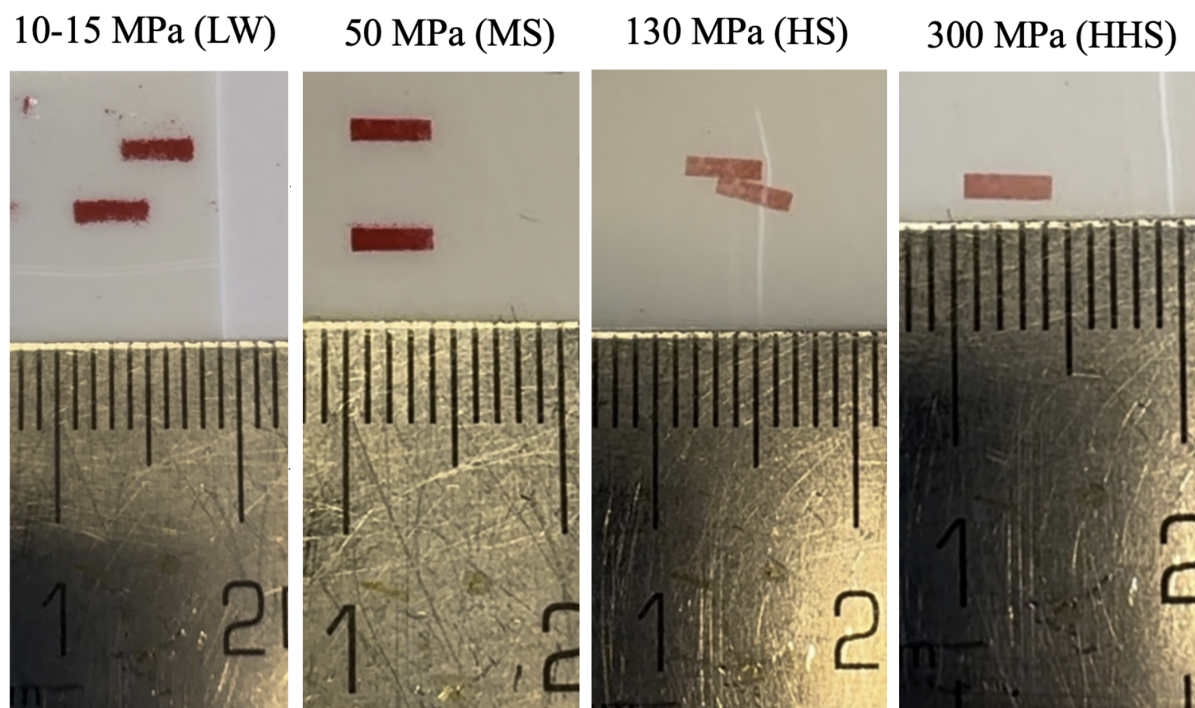


Figure 11: Final Bennie press homogeneity results (scale in mm).

As can be seen in Figure 11, reproducibility of homogeneous pressure distribution was achieved. The results are in accordance with the expectations for successful Bennie press homogeneity validation. Significantly reduced friction between wedge, sliding area and lever bottom surface could be the main contributor to the improved homogeneity and ensure that wedge stays aligned while moving upward. However, the unloading mechanism misbehaviour escalated. At the initial pressure distribution examination, gradual unloading could be achieved by additional hand pressure application. During the final homogeneity testing, the gradual unloading could not be accomplished anymore for pressures above 50 MPa. The unloading could only be done rapidly. If the unloading is sudden, due to the high stress concentration inside the tape, the sudden pressure release can affect ReBCO's atomic structure, thus, possibly damaging the superconductor layer. Taking into account the importance of gradual force release, a decision had to be made about whether to continue improving the unloading mechanism or design a new setup for the critical current against transverse stress at 77 K. The Bennie press was concluded to be unsuitable for the state-of-the-art ReBCO tape critical current against transverse stress measurements for the following reasons:

1. Sudden force release might damage the ReBCO tape during the critical current against transverse stress experiment;
2. Small range of sample measurement area limits the generality of the results;

3. Bennie press was not designed for the high stresses needed for ReBCO. Thus, it is sensitive to any adjustments made to achieve the necessary load limits for ReBCO;
4. Improving the gradual force release could affect the functionality of other press elements, thus complicating the solution;
5. Homogeneous pressure distribution at room temperature does not guarantee homogeneity at 77 K;
6. EMS had come across a new, affordable and strong hydraulic press advertised by Rintje Ritsma with a maximum capacity of 10 t [67]. In comparison, Bennie press maximum capacity is 0.6 t [62].

### Rintje Ritsma Press Design

Points 1 and 6 from the list above were the main deal-breakers for the next step in this research. Due to the large increase in the applied weight capacity for the Rintje Ritsma press and the expected maximum pressure application of 800 MPa (with safety margin), the sample area can be increased from 4 mm<sup>2</sup> to 120 mm<sup>2</sup>. Additionally, the press design ensures relatively reliable gradual force release at 77 K using a pump handle (Figure 12). The main challenges were to make an assembly that could measure the critical current against transverse stress under LN<sub>2</sub> (reproducibly) and have sufficiently uniform pressure distribution on the 30 times larger sample area than before. Combining these challenges with the design requirements mentioned in the methodology chapter, the final design of the Rintje Ritsma press is proposed (Figure 12).

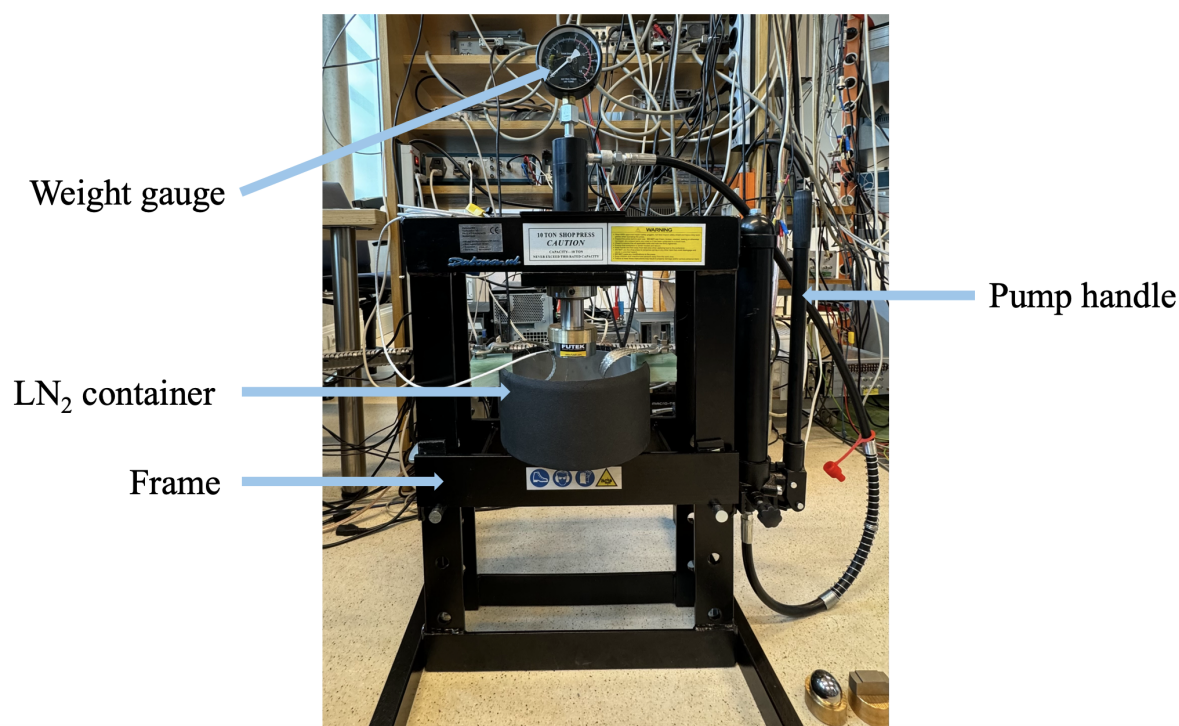
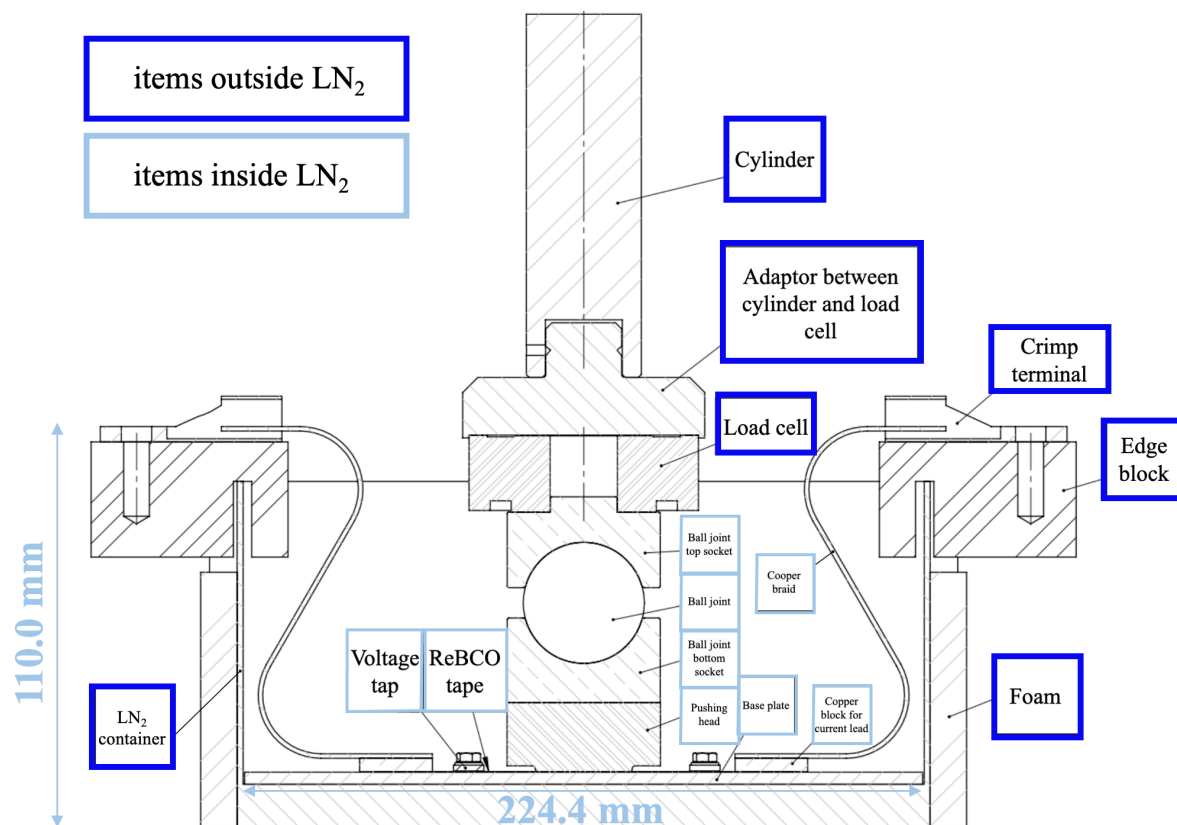


Figure 12: Rintje Ritsma press design (60x45x106 cm [67]).

The frame is mounted together with the pump handle and weight gauge. LN<sub>2</sub> is filled in the container, where the transverse stress experimental elements are assembled (Figure 13) and connected to the critical current measurement setup (Figure 9).



Note. A second pair of voltage taps was installed on both sides of the pushing block (35 mm distance) for the second sample measurement.

Figure 13: Critical current against transverse stress at 77 K measurement assembly.

Every assembly element has a specific function. The cylinder is connected to the hydraulic pump and moves down when force is applied. It moves gradually upwards when the force is released. It is a part of the frame setup. All items underneath the cylinder were manufactured at the TCO workshop or Superconductivity Laboratory or gathered from the previous EMS experiments. The adaptor (brass) between the cylinder and the load cell holds the two elements together. Brass was chosen because it is easy to machine while still exhibiting enough strength. The load cell measures the applied force. The crimp terminal is a connector between the current lead and the copper braid, which supplies current to the sample. The edge block holds on the side of the container as a base element for the crimp terminal. Edge blocks were made out of G11 due to the material's ability to resist cryogenic temperatures and act as an insulator. The elasometric foam (synthetic rubber) is glued around the stainless steel container for the researcher's safety to avoid cold burns if the container is accidentally touched during the experiment. The stainless steel container was provided by the TCO. The TCO chose stainless steel because it is easy to weld, making it possible to produce a leak-tight wall in a round shape. Inside the container, there is a 4 mm thick titanium base plate with a radius of 0.2 mm smaller than the container due to thermal compression. The tape sample, voltage taps, and copper blocks are bolted on the base plate. Voltage taps measure the potential difference between both sides of the pushing head. Copper blocks ensure charge carrier transport from copper braids into the sample. Copper was chosen due to its good conductivity. Indium foil is placed between the copper foil and the ReBCO tape to help them stick together. Copper foil is under a small piece of G11, which is stycasted at the bottom of the voltage tap plate seen in Figure 14. Copper wires are soldered underneath the copper foil. The voltage tap

assembly can be found in the appendix for more detail. Titanium pushing block has direct surface contact with the tape. Similarly to the Bennie press, it is a crucial contributor to homogeneous pressure application. Titanium was chosen for the pushing head and base plate to prevent plastic deformation from the high transverse loads expected during the experiment. The ball joint is responsible for the alignment due to its freedom to move in a circular motion.

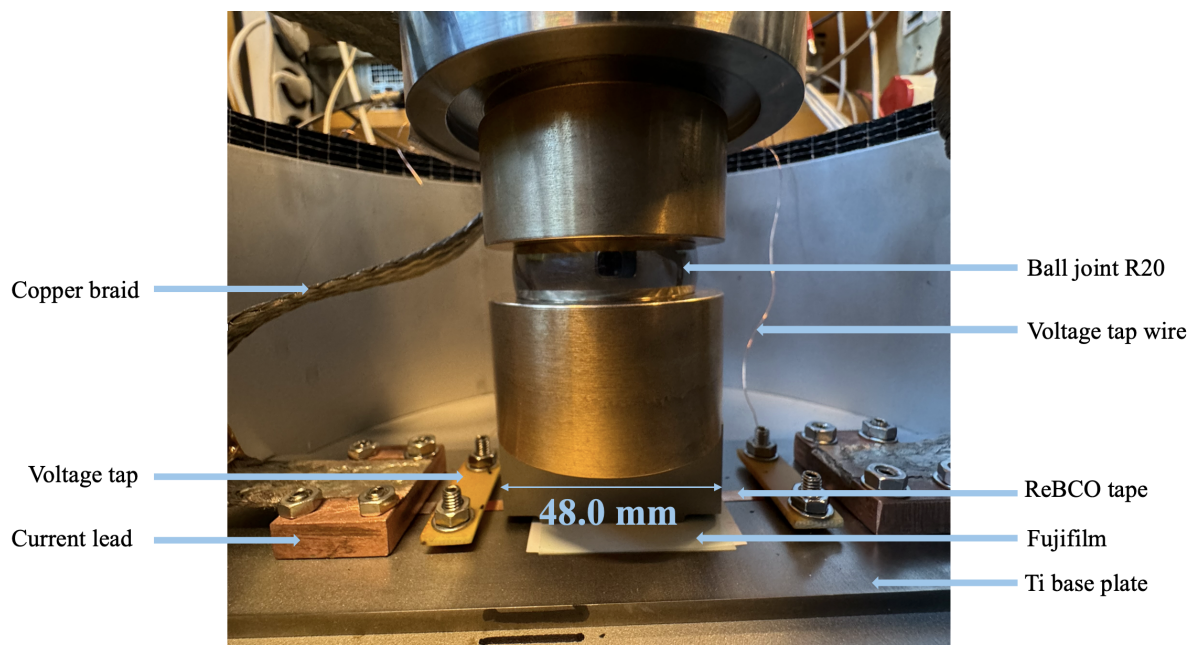


Figure 14: Cryogenic assembly.

Homogeneity of the setup was tested only with the MS film (indicated as "Fujifilm" in Figure 14) at room temperature to prevent damaging the installed ReBCO tape. According to the film results depicted in Figure 15, the homogeneity is sufficiently uniform. The conclusion is based on the similar colouring of the homogeneous pressure distribution in Figure 10 at 300 MPa.

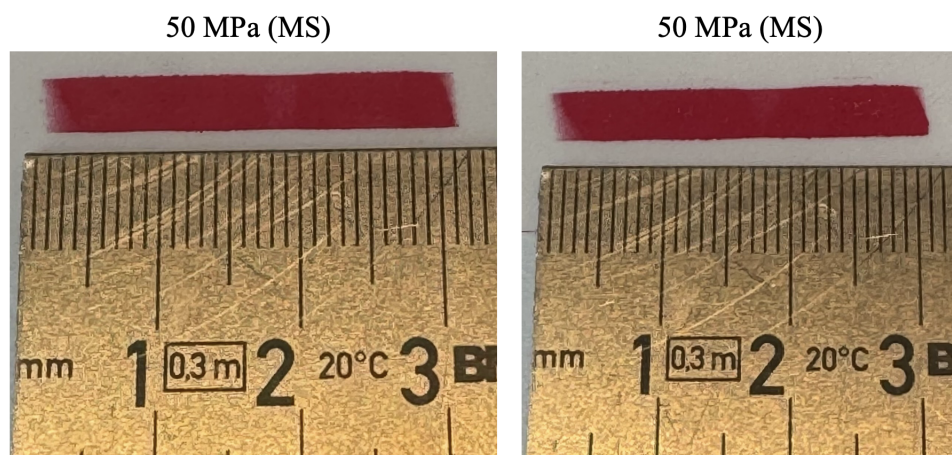
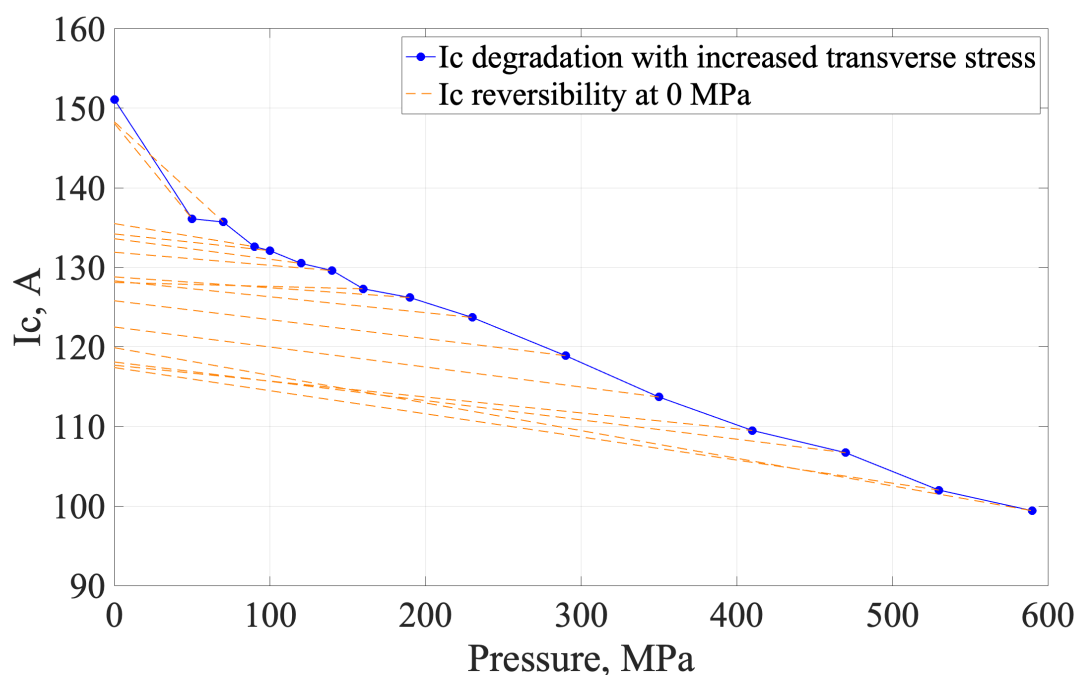


Figure 15: Rintje Ritsma press homogeneity at 50 MPa at room temperature.

## Critical Current Against Transverse Stress for Sample #1

The testing sample for all measurements was SuperOx 2513 4 mm wide and 55  $\mu\text{m}$  thick ReBCO tape with a 5  $\mu\text{m}$  thin Cu layer on each side, 2  $\mu\text{m}$  Ag layer, 2.5  $\mu\text{m}$  ReBCO layer, 0.2  $\mu\text{m}$  buffer layer, and 40  $\mu\text{m}$  thick substrate layer [68]. The main goal of the experiment is to measure the sample's critical current dependencies for the transversely applied force. The results for sample #1 are depicted in Figure 16. 600 MPa was the maximum transverse stress value due to the expected limit being in the range of 600-700 MPa. Thus, the anticipated graph should show a relatively parallel (up to 5%  $I_c$  variation is acceptable [69]) line along the pressure axis until around 600 MPa. The maximum of 700 MPa was not deemed necessary due to the significant degradation of current at lower pressures.



Note. 0 MPa is 0.16 MPa in reality due to the setup weight of 18.62 N.

Figure 16: Sample #1 critical current ( $I_c$ ) against transverse stress measurement results with Rintje Ritsma press.

The critical current value of sample #1 with a setup load of 18.62 N (0.16 MPa) was measured to be 151 A. From Figure 16, the following conclusions can be drawn about the critical current degradation and reversibility under transverse stress of the sample. At 50 MPa, the critical current degradation was already 10%, but after unloading,  $I_c$  value was reversed to 148 A (2% degradation). Similar results were obtained at 70 MPa transverse stress. Thus, concluding that the critical current degradation happened after the first load application. However, the unloading reversibility was achieved until 70 MPa. After exceeding 90 MPa, the critical current was irreversible and degrading at a slower rate than for smaller transverse stress values.

The sudden critical current drop before 90 MPa can be explained due to the misalignment of the pushing block that was observed after pouring  $\text{LN}_2$  for the first time. The load cell and adaptor were not tightly connected, thus shifting in the dynamic  $\text{LN}_2$  environment and displacing the pushing head. After warming up the setup, the position of the pushing block was examined (Figure 17). The pushing block was misaligned during the measurements, which might have caused an inhomogeneous pressure distribution. Marks on one side of the tape

surface support the assumption (Figure 18). Another observation of the cryogenic setup post-experiment indicates that the pushing head was touching the surface of the titanium plate (Figure 19). Initially, the pushing head was meant to touch only the surface of the sample. From there, it is clear that the pressure distribution was over a larger area than estimated, meaning that the pressure exerted on the sample was smaller. This observation could explain the shallow critical current degradation after 90 MPa.

The relative uncertainty regarding the critical current measurement was 0.1% and 16.2% for the force indication from the weight gauge. Additional error analysis was done for the pressure value, which yielded the same value as for the force. This allows to claim that the experimental error is equal for homogeneous and inhomogeneous pressure distributions. The experimental error in critical current measurement comes from the V-I software, which displays the current value from a power supply with a unit of 0.1 A. The large experimental force uncertainty is due to the instrument units. The applied force was determined from a weight gauge, which had the smallest unit of 1 t, allowing to assume the absolute uncertainty as half of this value [70]. Even though the experimental error of force identification is relatively large, the relationship between the critical current and pressure seems to be mostly systematic, and due to time constraints, the measuring equipment will not be considered a reason for the unexpected results.

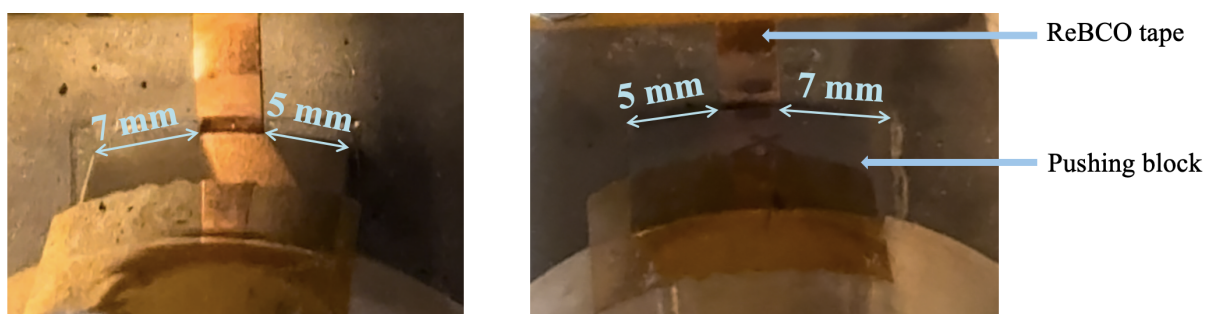


Figure 17: Position of one side (left) of pushing block and position of the other side (right) of pushing block with respect to sample #1 at room temperature after measurements [top view].

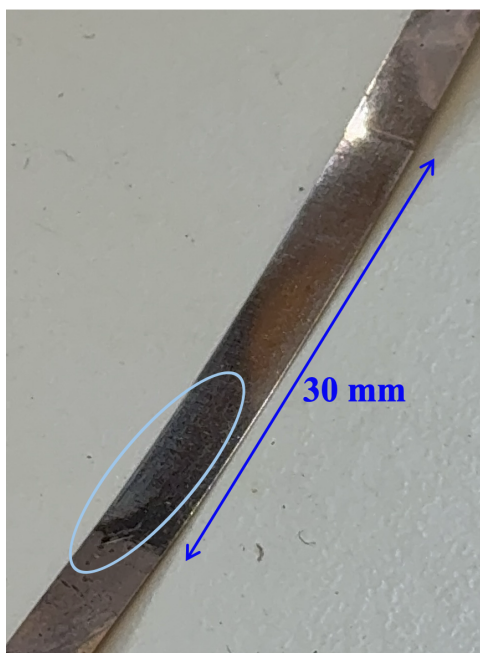


Figure 18: ReBCO sample #1 surface after the experiment.

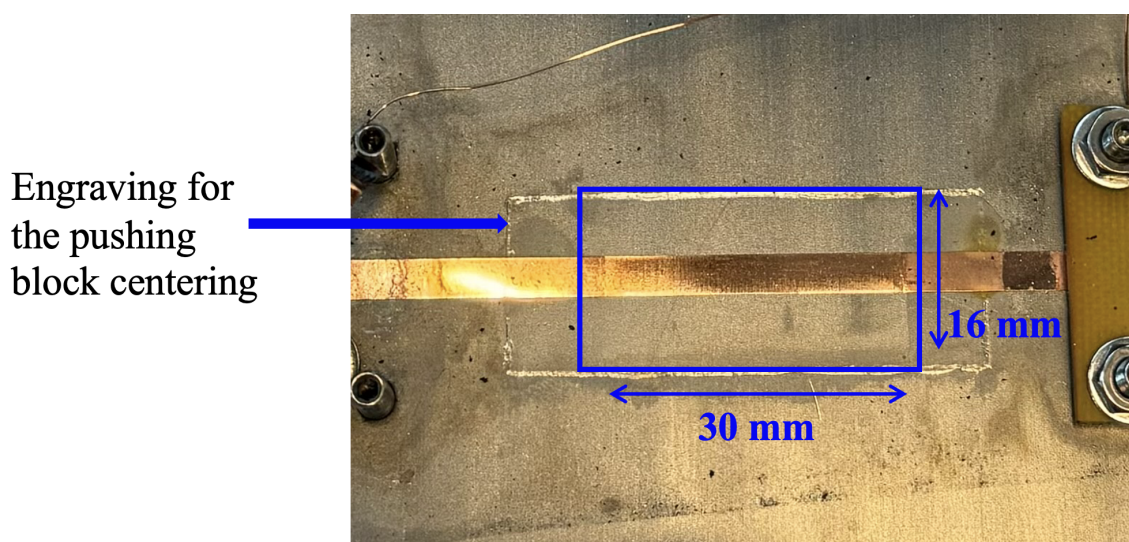


Figure 19: Pushing head marks on the Ti plate after the experiment.

### Critical Current Against Transverse Stress for Sample #2

To minimise the influence of the pushing block misalignment on the critical current dependency under transverse stress, the pushing block was secured to the titanium plate using kapton tape. Next to that, a negligible mass (around 0.1 t) was applied to the cryogenic assembly to ensure contact between the adaptor and the load cell. The contact is essential for the structural stability during LN<sub>2</sub> pouring. Additionally, a second pair of voltage taps was added closer to the pushing block to exclude voltage measured through the non-experimental section of the tape. However, the results depicted in Figure 21 are drawn only from the voltage taps closer to the copper blocks. For now, the other voltage tap pair readings are disregarded to simplify the result comparison between sample #1 and sample #2. This can be done because the results were similar among the voltage tap pairs. The only difference



was an insignificant, distinct reference point.

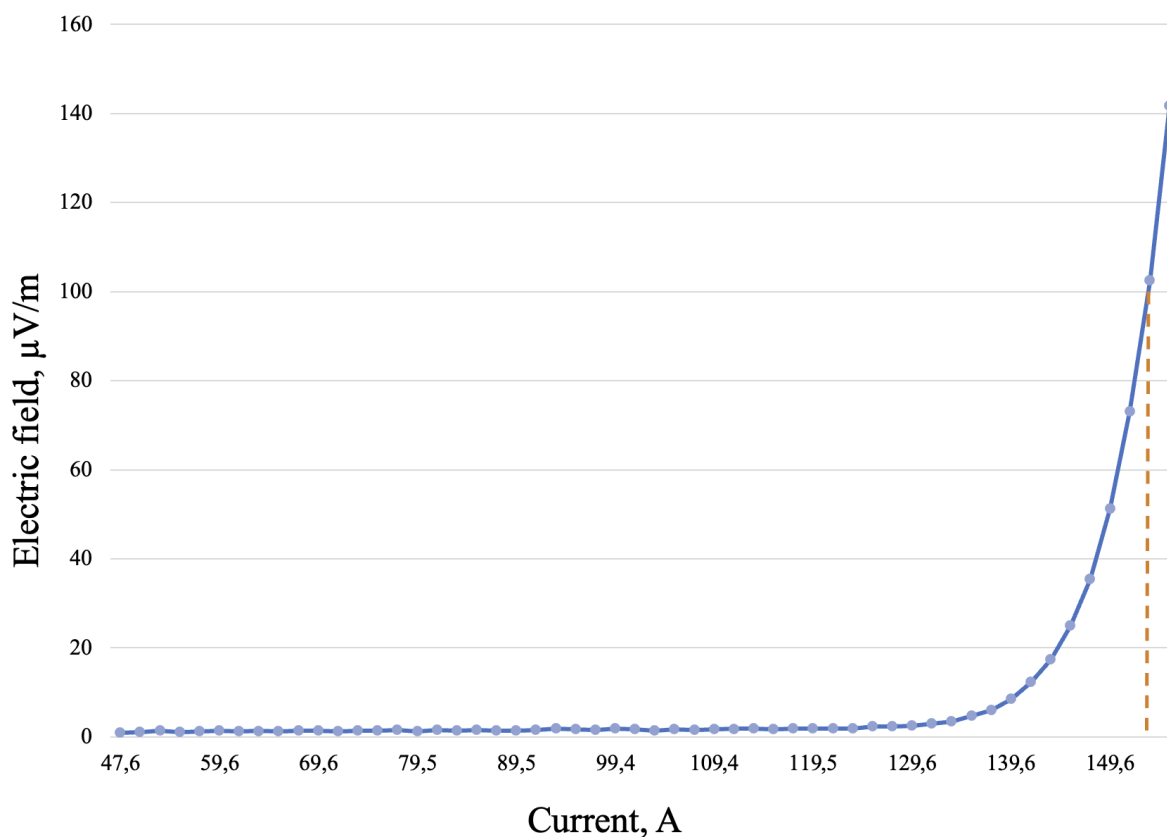


Figure 20: Critical current identification of sample #2 using the electrical field criterion of  $100 \mu\text{V m}^{-1}$  with pre-load.

From Figure 20, the obtained critical current value for sample #2 with pre-load was 152.8 A. The data point slightly above  $100 \mu\text{V m}^{-1}$  is a signal delay between the voltmeter and power supply. After the measurement, the precise critical current at  $100 \mu\text{V m}^{-1}$  was calculated in the V-I program. The critical current 5% variation was considered until 145.1 A. The electric field was calculated by considering the larger voltage tap distance of 73 mm to simplify the result comparison between the two samples. The obtained results for the critical current against transverse stress are shown in Figure 21.

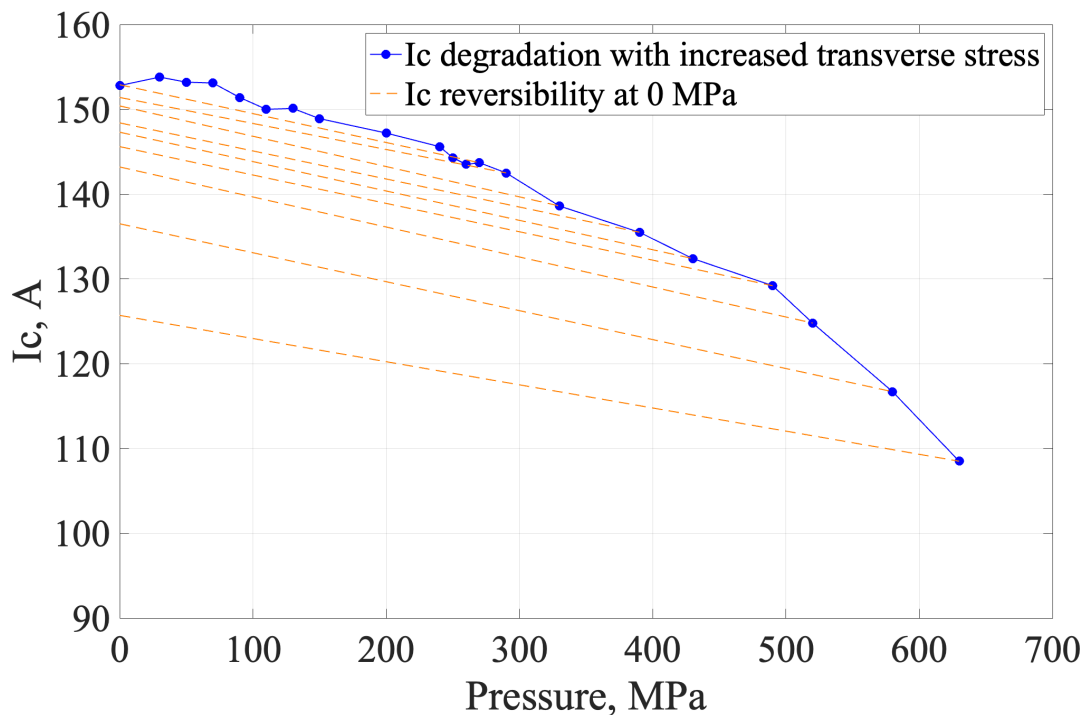


Figure 21: Sample #2 critical current ( $I_c$ ) against transverse stress measurement results with Rintje Ritsma press.

The results show negligible ( $< 5\%$ ) critical current degradation until 240 MPa transverse stress. A significant critical current drop happened between 270 MPa and 330 MPa, where degradation increased by 4%. A similar observation can be made about the steep critical current degradation between stresses of 490 MPa and 520 MPa. Interestingly, the critical current was reversed within the acceptable range (5%) until 490 MPa.

Similarly to sample #1 results, the behaviour of the graph will be described based on the possible flaws in the setup rather than the measurement accuracy. The experimental error of critical current measurement was 0.1% and for force determination 14.9%. The relatively significant decrease in critical current between 270 MPa and 330 MPa was possibly due to an accidental movement of the press frame while applying the force. The displacement of the press frame could have exerted more force on the sample, possibly damaging it. Afterwards, it is difficult to anticipate any specific critical current degradation behaviour due to the uncertainty regarding the extent of damage to the sample.

## Critical Current Against Transverse Stress Result Comparison Between Sample #1 and Sample #2

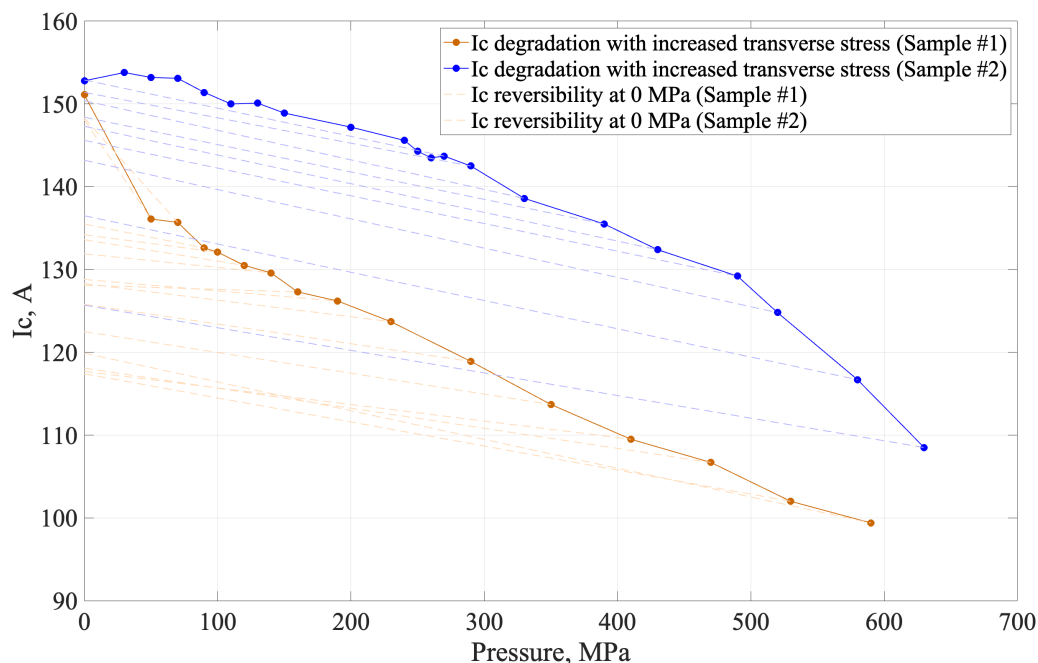


Figure 22: Sample #1 and sample #2 critical current ( $I_c$ ) against transverse stress measurement results with Rintje Ritsma press.

The two graphs showcase very different behaviours. In general, the rate of critical current decrease for sample #2 is slower than for sample #1. This can be explained by the inhomogeneous pressure distribution on sample #1 since the beginning of the measurements analysed above. The position of the pushing block and the homogeneity of the sample #2 surface were also examined after the experiment (Figure 23 and 24). Before the experiment, the pushing block was centred. However, after the experiment, it appeared to have drifted to the left side. The displacement may have happened after the accidental pushing of the frame before 330 MPa and 490 MPa applications. That also explains why the rate of critical current decrease accelerated after the frame movement. No additional marks were observed on sample #2 in comparison to sample #1 after the experiment. However, after both sample measurements, the pushing head marks were visible on the Ti plate, supporting the assumption that the exerted force on the sample was less than expected. If the force is equally distributed over the entire surface, the pressing area increases 4 times, thus, the pressure applied to the sample is 4 times less than expected. Overall, the additional stability of the cryogenic assembly applied before sample #2 critical current against transverse stress measurement has had a significant impact on the critical current degradation. Thus, supporting the claim that result accuracy depends on the setup alignment.

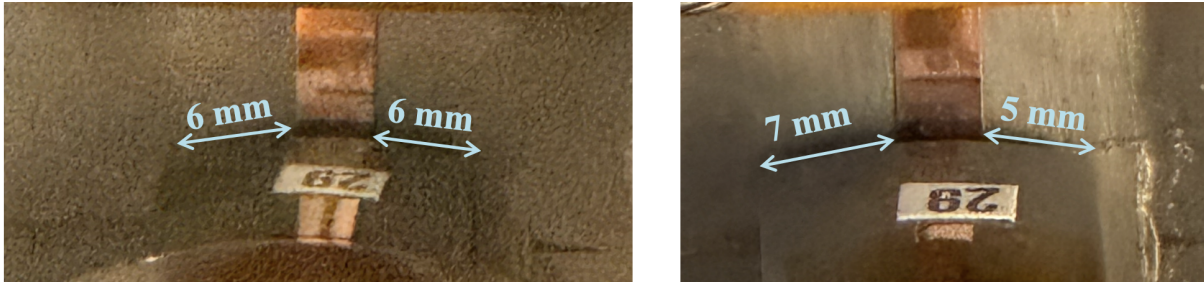


Figure 23: The position of one side of the pushing block with respect to the sample #2 before (left) and after (right) the experiment.

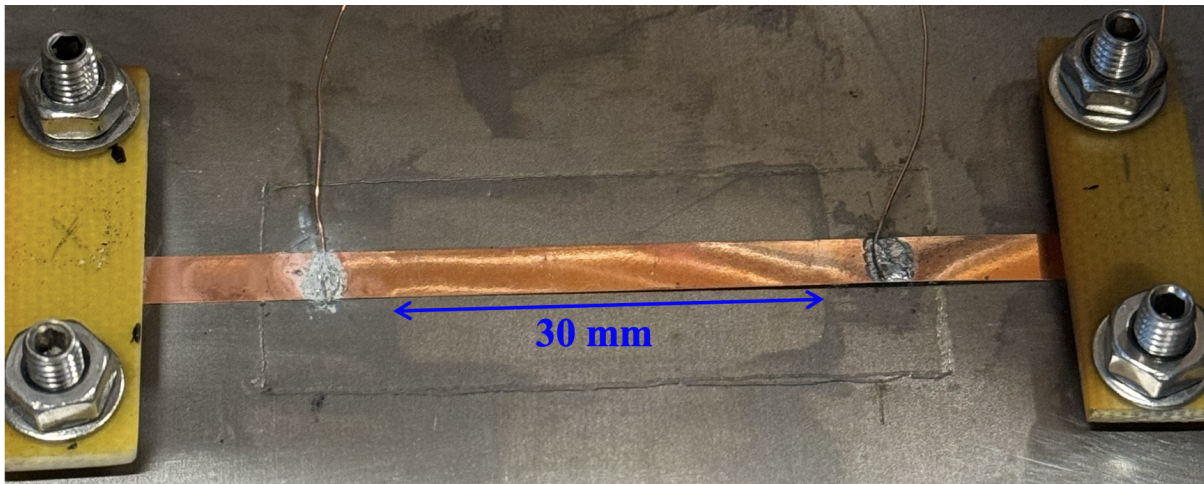


Figure 24: Sample #2 surface and pushing head marks on the Ti plate after the experiment.

# Outlook

## Limitations of the Bennie Press Homogeneity Examination

Even though the Bennie press was determined to be unsuitable for the state-of-the-art ReBCO coated conductor critical current against transverse stress at 77 K measurements, mainly due to the faulty unloading mechanism, its functionality was never checked at the cryogenic temperature. The possibility of improved performance is small. Nevertheless, it cannot be claimed that the mechanism will not work properly without real data at 77 K with the new bronze wedge and polished surfaces.

## Limitations of the Rintje Ritsma Press Design

Rintje Ritsma press design has several limitations. The maximum transverse stress area is 120 mm<sup>2</sup>, which is still little compared to the surface area of the magnet coils that would be exposed to the transverse stresses during pre-stressing. Thus, it would still be difficult to generalise the results of this press setup for coil applications. The experimental surface area is constrained by the maximum capacity of the hydraulic press (10 t). Next to that, the pushing head width (16 mm) is larger than the width of the sample (4 mm). Because the ReBCO tape is softer than the titanium pushing head, it makes contact with the titanium base plate surface around the sample. This behaviour leads to less pressure exerted on the sample than expected, leading to imprecise quantitative results. Additionally, the homogeneity of the press was only verified up to 50 MPa due to the possibility of sample damage. A different obstacle is that the load cell is affected by the LN<sub>2</sub> which changes its mechanical and electrical properties. The load cell showed different output every time it was incorporated into the cryogenic setup (Figure 25). Additionally, the linearity coefficient of the three graphs above LN<sub>2</sub> was not a constant, making it difficult to draw accurate values. This behaviour could be explained by the different temperatures of the load cell during the measurements since the element is not under LN<sub>2</sub>. Unfortunately, the different temperatures were not measured, and this is an assumption. Thus, the load cell was not used for pressure determination. Instead, a weight gauge on top of the press frame was used, which contributed to a relatively large experimental error.

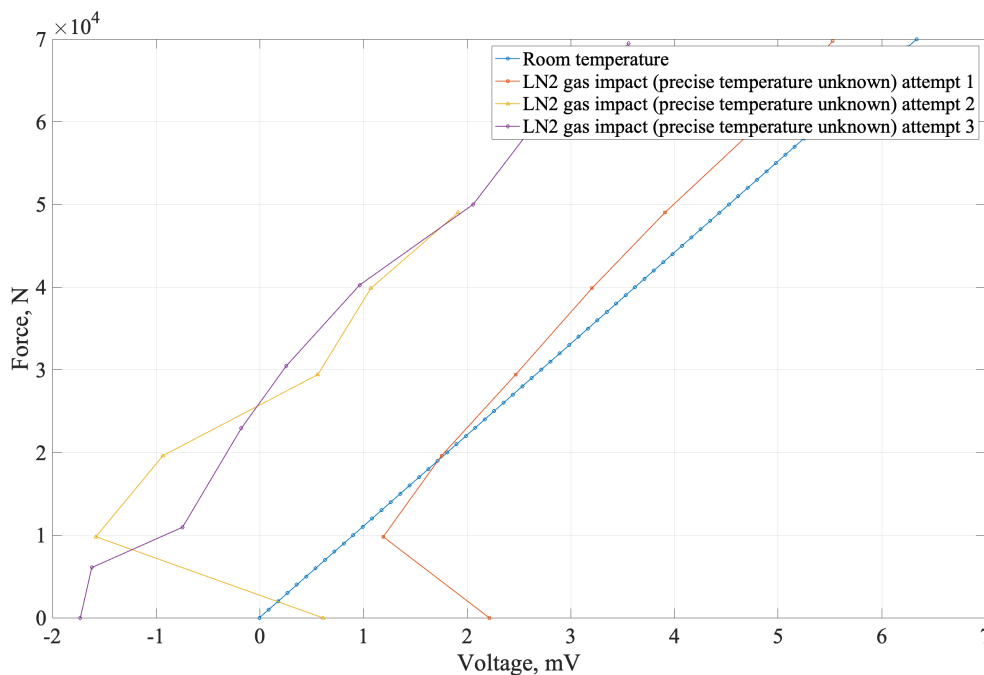


Figure 25: Load cell calibration at room temperature versus above the LN<sub>2</sub>.

Another limitation arises because the titanium base plate has a radius 0.2 mm smaller than the container, allowing slight movement inside the container. Every time the sample is changed, the plate is positioned differently. This means that the alignment of the container must be tested after every sample installation. Finally, applying more than 50000 N to the sample is physically difficult due to the resistance. This is an important limitation, since failure to apply the force in a uniform and steady way can result in undesired displacement of the press frame. It was assumed to have the largest impact on sample #2 critical current against transverse stress results.

Overall, the most essential limitations of the Rintje Ritsma measurement setup are the high possibility of misalignment due to loose cryogenic elements, pushing head touching the titanium base plate area, and the load cell calibration. The cryogenic assembly can be relatively easily misaligned during the measurement if it is not properly fixed in a centred position. Moreover, for increased result accuracy, the pushing head must make surface contact only with the sample, and the load cell needs to be adequately utilised. Possible solutions for these challenges are discussed in the following section.

### Implications for Future Research with the Rintje Ritsma Press

Future research on ReBCO critical current against transverse stress should be continued with the Rintje Ritsma press due to the increased experimental area and potential reliability. However, several press components must be further investigated and improved.

Ensuring the pushing head alignment and centering throughout the experiment is crucial. It must be able to tolerate the dynamic LN<sub>2</sub> environment and other possible disturbances during the experiment. The stability can be improved if the pushing head width is reduced to some value close to the ReBCO tape width, for instance, 4.1 mm. That way, the pushing head stays only on top of the sample and it has limited freedom to shift to either side.

Additionally, that would resolve the larger pressure area challenge. The currently used pushing head with a 16 mm width can be stabilised by mounting another piece of ReBCO tape on both sides of the experimental sample. That would also constrain the pushing block to shift to one side, a behaviour best seen in Figure 17. However, a limitation of this approach is that higher loads will be needed to achieve the desired pressures, possibly exceeding the maximum capacity of the press.

The load cell must either be calibrated and used at 77 K or it must be thermally insulated from the cryogenic assembly. If the load cell is calibrated at 77 K, a new container will be needed since the walls of the current container are not high enough to contain the LN<sub>2</sub> up to the position of the load cell. Alternatively, thermal insulation of the load cell can be attempted by applying either a heater or a material with low thermal conductivity (G11, kapton, or plastic) cover layer to the bottom of the load cell. Thus, limiting thermal conductivity from the assembly items under the LN<sub>2</sub>. This approach allows for the use of load cell calibration data at room temperature.

Moreover, the press frame could be mounted to the ground to avoid possible press movement, which might hinder the cryogenic assembly alignment. Another option is to support the press from both sides with additional weight. Once the mechanical obstacles are resolved to a sufficient level, the reproducibility of the results must be investigated. Only then can the Rintje Ritsma press critical current against transverse stress results be validated. Finally, it is essential to consider the possibility that the ReBCO tape samples do not exhibit the mechanical limitations that are expected in these transverse load experiments. If the sample is defective, it may plastically deform under lower pressures. In that case, the edges of the pushing block radius may apply additional stresses that can influence the critical current against transverse stress results. Thus, the experimental tapes need to be studied on a microscopic level to identify any possible manufacturing deficiencies.

## Contextual Exploration

There are three main research outcomes. Firstly, Bennie press is unsuitable for the state-of-the-art ReBCO tape critical current against transverse stress measurements. Secondly, a new press design was proposed - the Rintje Ritsma press, which allows for a larger measurement area, homogeneous pressure distribution, and gradual unloading. Thirdly, the quantitative results with the Rintje Ritsma press currently show that the mechanical strength of the state-of-the-art ReBCO tape with 5 µm Cu stabiliser thickness is 240 MPa at 4.7% critical current degradation. However, this result should not be regarded accurate yet. The Rintje Ritsma press has numerous mechanical challenges that must be resolved before generalising any quantitative results. Once the design is finalised and repeatable experiments are executed, EMS will have obtained a reliable result of the ReBCO transverse stress limit. Together with other Lorentz force component limitations currently being researched at the EMS, whole data set for ReBCO mechanical boundaries can be presented to the partnering institutions. Furthermore, using these results, joint efforts can be made to research the possibility of coil pre-stressing, which prevents delamination [61]. If that is successful, a mitigation for one of the biggest technical concerns of the ReBCO tape is achieved. Once quality control has taken a step forward, further developments towards ReBCO commercialisation can take place. For large scale application, ReBCO cost reduction is mandatory [71]. ReBCO performance improvements can increase demand. If the demand increases to 1000s of km per year, the production cost are expected to decrease to the levels required for widespread applications, including compact fusion reactors [7]. Development of compact fusion reactors may benefit society greatly. In general, fusion provides continuous electricity production without

relying on environmental limitations, such as wind or the sun. Radiological safety is the primary advantage of fusion over fission. However, the outstanding thing about the CFR is its ability to deploy the reactor wherever it is needed to facilitate energy demand, including remote places unsuitable even for fossil fuel power stations [72].



## Conclusion

Research on the critical current against transverse stress of the state-of-the-art ReBCO tape was carried out by considering two different press setups. The initial Bennie press homogeneity examination showed occasional inhomogeneous pressure distribution together with a faulty unloading mechanism. The final Bennie press homogeneity examination yielded sufficient homogeneity. However, the Bennie press was concluded to be unsuitable for the critical current against transverse stress measurements for the state-of-the-art ReBCO tape, mainly due to its mechanical malfunction. Gradual unloading of the transverse stress was not achieved with the Bennie press. Alternatively, a new press setup was designed for the critical current against transverse stress measurements for the state-of-the-art ReBCO tape. The Rintje Ritsma press allows for a larger experimental area, gradual force release, and homogeneous pressure application, among other benefits. Sample #1 results showed no transverse stress limit. After improving the stability of the Rintje Ritsma setup, the transverse stress limit with the applied load was found to be 240 MPa at 4.7% critical current degradation for the sample #2. Moreover, reversible current was achieved until 490 MPa at 4.7% critical current degradation. However, there are several improvements to be made to the Rintje Ritsma setup to possibly improve the results. The press frame must be stabilised to the ground to avoid any movement during force application, the pushing head must be secured to ensure homogeneous pressure distribution over the sample area, and the load cell should either be calibrated and used at 77 K or thermally insulated from the cryogenic assembly. If the mechanical limitations are mitigated and the reproducibility of the results is obtained, the critical current against transverse stress results with the Rintje Ritsma press can be validated.

## References

- [1] M. Chersich, N. Brink, M. Craig *et al.*, “A WHO-led global strategy to control greenhouse gas emissions: a call for action,” *Global Health*, vol. 20, no. 4, 2024. [Online]. Available: <https://doi.org/10.1186/s12992-023-01008-6>
- [2] S. Speller, “Can superconductors help us save the planet?” July 2022. [Online]. Available: <https://www.youtube.com/watch?v=BkFWic9gv8w>
- [3] H. Jones, “Superconductors in the transmission of electricity and networks,” *Energy Policy*, vol. 36, no. 12, 2008. [Online]. Available: <https://www.sciencedirect.com/science/article/pii/S0301421508004473>
- [4] P. Sutter, “What is a superconductor?” July 2021. [Online]. Available: <https://www.livescience.com/superconductor>
- [5] Y. Chen, L. Fu, X. Chen, S. Jiang, X. Chen, J. Xu, and B. Shen, “Ultra-low electrical loss superconducting cables for railway transportation: Technical, economic, and environmental analysis,” *Journal of Cleaner Production*, vol. 445, 2024. [Online]. Available: <https://www.sciencedirect.com/science/article/pii/S0959652624007571>
- [6] A. P. Malozemoff, S. Fleshler, M. Rupich, C. Thieme, X. Li, W. Zhang, and H.-W. Neumueller, “Progress in high temperature superconductor coated conductors and their applications,” *Superconductor Science and Technology*, vol. 21, no. 3, 2008.
- [7] N. C. Mitchell, J. Zheng, C. Vorpahl, V. Corato, C. Sanabria, M. Segal, B. Sorbom, R. Slade, G. D. Brittles, R. Bateman, Y. Miyoshi, N. Banno, K. Saito, A. Kario, H. J. ten Kate, P. Bruzzone, R. Wesche, T. Schild, N. Bykovskiy, and A. Dudarev, “Superconductors for fusion: a roadmap,” *Superconductor Science and Technology*, vol. 34, no. 10, 2021.
- [8] Y. Zhai, C. Kessel, C. Barth, and C. Senatore, “High-performance superconductors for Fusion Nuclear Science Facility,” *IEEE Transactions on Applied Superconductivity*, vol. 27, no. 4, 2016.
- [9] X. Zhang, M. Xu, Z. Chen, X. Yang, T. Zhao, R. Ye, X. Yang, X. Bian, Y. Gao, H. Lu, R. Ge, Z. Zhu, and Y. Li, “Development of a superconducting undulator cryostat based on the thermosiphon effect,” *International Journal of Refrigeration*, vol. 164, 2024. [Online]. Available: <https://www.sciencedirect.com/science/article/pii/S0140700724001634>
- [10] A. Nordrum, “The era of cheap helium is over—and that’s already causing problems,” February 25 2024. [Online]. Available: <https://www.technologyreview.com/2024/02/25/1088930/global-helium-market-semiconductors/>
- [11] Z. Johal. (2021, March) Us researchers design compact fusion power plant. General Atomics. [Online]. Available: <https://www.ga.com/us-researchers-design-compact-fusion-power-plant>
- [12] ITER, “Magnets,” 2015. [Online]. Available: <https://www.iter.org/mach/Magnets>

- [13] J. E. Menard, “Compact steady-state tokamak performance dependence on magnet and core physics limits,” *Philosophical Transactions of the Royal Society A*, vol. 377, 2019. [Online]. Available: <https://doi.org/10.1098/rsta.2017.0440>
- [14] D. Whyte, J. Minervini, and B. e. a. LaBombard, “Smaller sooner: Exploiting high magnetic fields from new superconductors for a more attractive fusion energy development path,” *Journal of Fusion Energy*, vol. 35, no. 1, pp. 41–53, 2016.
- [15] S. Woodruff, J. K. Baerny, N. Mattor, D. Stoullil, R. Miller, and T. Marston, “Path to market for compact modular fusion power cores,” *Journal of Fusion Energy*, vol. 31, no. 4, pp. 305–316, 2011. [Online]. Available: <https://doi.org/10.1007/s10894-011-9472-6>
- [16] S. Erim, V. Chauvet, and D. Heger, “Follow up study on the economic benefits of iter and ba projects to eu industry,” 2021.
- [17] E. Hussein, “Emerging small modular nuclear power reactors: A critical review,” *Physics Open*, vol. 5, 2020.
- [18] D. X. Fischer, “How fusion brings high-temperature superconductors into the energy industry,” 2021.
- [19] K. Ilin, K. A. Yagotintsev, C. Zhou, P. Gao, J. Kosse, S. J. Otten, W. A. J. Wessel, T. J. Haugan, D. C. van der Laan, and A. Nijhuis, “Experiments and FE modeling of stress–strain state in ReBCO tape under tensile, torsional and transverse load,” *Superconductor Science and Technology*, vol. 28, no. 5, 2015.
- [20] L. Pentenga, A. Kario, S. Otten, S. Wessel, and R. Lubkemann, “Transverse stress single tapes,” February 2024.
- [21] A. Cheung, “High temperature superconductors and energy from fusion,” <http://large.stanford.edu/courses/2019/ph241/cheung2/>, [Lecture material from Stanford University course PH241].
- [22] A. von Meier, *Electric Power Systems*. John Wiley & Sons, 2006.
- [23] M. Tinkham, *Introduction to Superconductivity*, ser. Dover Books on Physics Series. Dover Publications, 2004. [Online]. Available: <https://books.google.nl/books?id=VpUk3NfwDIkC>
- [24] S. Askenazy, L. V. Bockstal, F. Herlach, and H. J. Schneider-Muntau, “Pulsed field coils with optimized current density distribution,” *Measurement Science and Technology*, vol. 4, no. 10, October 1993.
- [25] A. M. Wolsky, R. F. Giese, and E. J. Daniels, “The new superconductors,” *Scientific American*, vol. 260, no. 2, 1989.
- [26] J. W. Lynn, *High Temperature Superconductivity*, ser. Graduate Texts in Contemporary Physics. Berlin: Springer-Verlag, 1990.
- [27] M. Ladd, H. Quick, O. Speck, M. Bock, A. Doerfler, M. Forsting, J. Hennig, B. Ittermann, H. Möller, A. Nagel, T. Niendorf, S. Remy, T. Schaeffter, K. Scheffler, H.-P. Schlemmer, S. Schmitter, L. Schreiber, N. Shah, T. Stoecker, and M. Zaitsev, “Germany’s journey toward 14 Tesla human magnetic resonance,” *Magma (New York, N.Y.)*, vol. 36, 04 2023.

- [28] C. Zhou, K. A. Yagotintsev, P. Gao, T. J. Haugan, D. C. van der Laan, and A. Nijhuis, "Critical current of various REBCO tapes under uniaxial strain," *IEEE Transactions on Applied Superconductivity*, vol. 26, no. 4, 2016.
- [29] C. Senatore, M. Alessandrini, A. Lucarelli, R. Tediosi, D. Uglietti, and Y. Iwasa, "Progresses and challenges in the development of high-field solenoidal magnets based on RE123 coated conductors," *Superconductor Science and Technology*, vol. 27, no. 10, 2014.
- [30] W. Zhou, R. Jia, J. Cao, and R. Liang, "Elastoplastic mechanical behavior of high-field magnet of rebco high temperature superconducting composite tape under extreme environment," *Composite Structures*, vol. 329, 2024. [Online]. Available: <https://www.sciencedirect.com/science/article/pii/S0263822323011522>
- [31] R. Pearson, M. Bluck, and S. Murphy, "A symbiotic approach to compact fission and fusion reactors," *Transactions of the American Nuclear Society*, vol. 117, pp. 378–381, 11 2017.
- [32] Y. Sarazin, J.-L. Duchateau, X. Garbet, R. Ghendrih, J. Guirlet, B. Hillairet, A. Pégourié, R. Torre, and R. Varennes, "Impact of the aspect ratio on tokamak reactor design," in *IAEA FEC 2021 - The 28th IAEA Fusion Energy Conference*, Nice (Virtual conference), France, May 2021. [Online]. Available: <https://cea.hal.science/cea-03253732>
- [33] A. Costley and S. McNamara, "Fusion performance of spherical and conventional tokamaks: implications for compact pilot plants and reactors," *Plasma Physics and Controlled Fusion*, vol. 63, no. 3, 2021.
- [34] C. Bachmann, M. Siccino, A. Ciula, P. Fanelli, G. Federici, L. Giannini, C. Luongo, P. Pereslavtsev, X. Sarasola, T. Steinbacher, and H. Zohm, "Re-design of eu demo with a low aspect ratio," *Fusion Engineering and Design*, vol. 204, 2024. [Online]. Available: <https://www.sciencedirect.com/science/article/pii/S0920379624003715>
- [35] J. E. Menard, "Compact steady-state tokamak performance dependence on magnet and core physics limits," *Philosophical Transactions of the Royal Society A: Mathematical, Physical and Engineering Sciences*, vol. 377, no. 2141, 2019.
- [36] C. Liu, Y. Shi, C. Liu, S. Tao, F. Liu, S. Chen, H. Xia, J. Zhou, and X.-Y. Zhang, "National round robin test (RRT) for delamination strength testing YBCO HTS wires at room temperature (RT) and 77K," *Physica Scripta*, vol. 98, no. 8, July 2023.
- [37] J. G. Weisend, "Cryocoolers," 2021. [Online]. Available: <https://uspas.fnal.gov/materials/21onlineSBU/Cryo/2021%20USPAS%20Lecture%2020.pdf>
- [38] MAGLAB, "Critical current density versus applied magnetic field for lts and hts," 2018. [Online]. Available: [https://nationalmaglab.org/media/i3chrqnf/je\\_vs\\_b-041118\\_1024x743\\_pal.png](https://nationalmaglab.org/media/i3chrqnf/je_vs_b-041118_1024x743_pal.png)
- [39] G. Succi, A. Ballarino, S. C. Hopkins, C. Barth, and Y. Yang, "Magnetic field and temperature scaling of the critical current of REBCO tapes," *IEEE Transactions on Applied Superconductivity*, vol. 34, no. 3, 2024.

- [40] X. Wang, S. A. Gourlay, and S. O. Prestemon, "Dipole magnets above 20 tesla: Research needs for a path via high-temperature superconducting rebco conductors," *Instruments*, vol. 3, no. 4, 2019. [Online]. Available: <https://www.mdpi.com/2410-390X/3/4/62>
- [41] P. Ebermann, "Relevance of the irreversible degradation of superconducting nb3sn wires and cables caused by transverse stress at room temperature within the fcc study at cern," May 2020.
- [42] R. N. Bhattacharya and M. P. Paranthaman, *High Temperature Superconductors*. John Wiley & Sons, 2011.
- [43] J. Ma, "Flux pumping for no-insulation high temperature superconducting rebco magnets," Ph.D. dissertation, University of Cambridge, 2020, apollo - University of Cambridge Repository. [Online]. Available: <https://doi.org/10.17863/CAM.58564>
- [44] C. Barth, G. Mondonico, and C. Senatore, "Electro-mechanical properties of REBCO coated conductors from various industrial manufacturers at 77 k, self-field and 4.2 k, 19 t," *Superconductor Science and Technology*, vol. 28, February 2015.
- [45] T. Benkel, Y. Miyoshi, X. Chaud, A. Badel, and P. Tixador, "REBCO tape performance under high magnetic field," *The European Physical Journal Applied Physics*, vol. 79, no. 3, 2017.
- [46] H. Ten Kate, A. Kario, and S. Otten, "ReBCO superconductor mechanical properties," 2023. [Online]. Available: <https://indico.cern.ch/event/1220254/contributions/5270725/attachments/2608381/4506334/20230309-TenKate%20-%20ReBCO%20Mechanical%20Properties.pdf>
- [47] H. Ten Kate, "Superconducting magnets quench propagation and protection," in *CERN Accelerator School on Superconductivity for Accelerators*, 2013. [Online]. Available: [https://indico.cern.ch/event/194284/contributions/1472819/attachments/281522/393603/TenKate\\_-\\_CAS\\_-Handout-Quench-Erice-2103.pdf](https://indico.cern.ch/event/194284/contributions/1472819/attachments/281522/393603/TenKate_-_CAS_-Handout-Quench-Erice-2103.pdf)
- [48] U. Floegel-Delor, T. Riedel, R. Rothfeld, P. Schirrmeister, R. Koenig, and F. N. Werfel, "High-efficient copper shunt deposition technology on rebco tape surfaces," *IEEE Transactions on Applied Superconductivity*, vol. 26, no. 3, 2016.
- [49] Y. Xu and D. Shi, "A review of coated conductor development," *Tsinghua Science and Technology*, vol. 8, January 2003.
- [50] D. Huang, H. Gu, H. Shang, T. Li, B. Xie, Q. Zou, and F. Ding, "Achievement of low-resistivity diffusion joint of REBCO coated conductors by improving the interface connection of Ag stabilizer," *IEEE Transactions on Applied Superconductivity*, vol. 31, no. 3, 2021.
- [51] A. Goyal and S.-H. Wee, "Buffer layers for REBCO films for use in superconducting devices," 2014.
- [52] M. Pu, G. Li, X. Du, Y. Zhang, H. Zhou, R. Sun, Z. Wang, and Y. Zhao, "A new series of potential buffer layers for rebco coated conductor," *Materials Science Forum - MATER SCI FORUM*, vol. 546-549, May 2007.

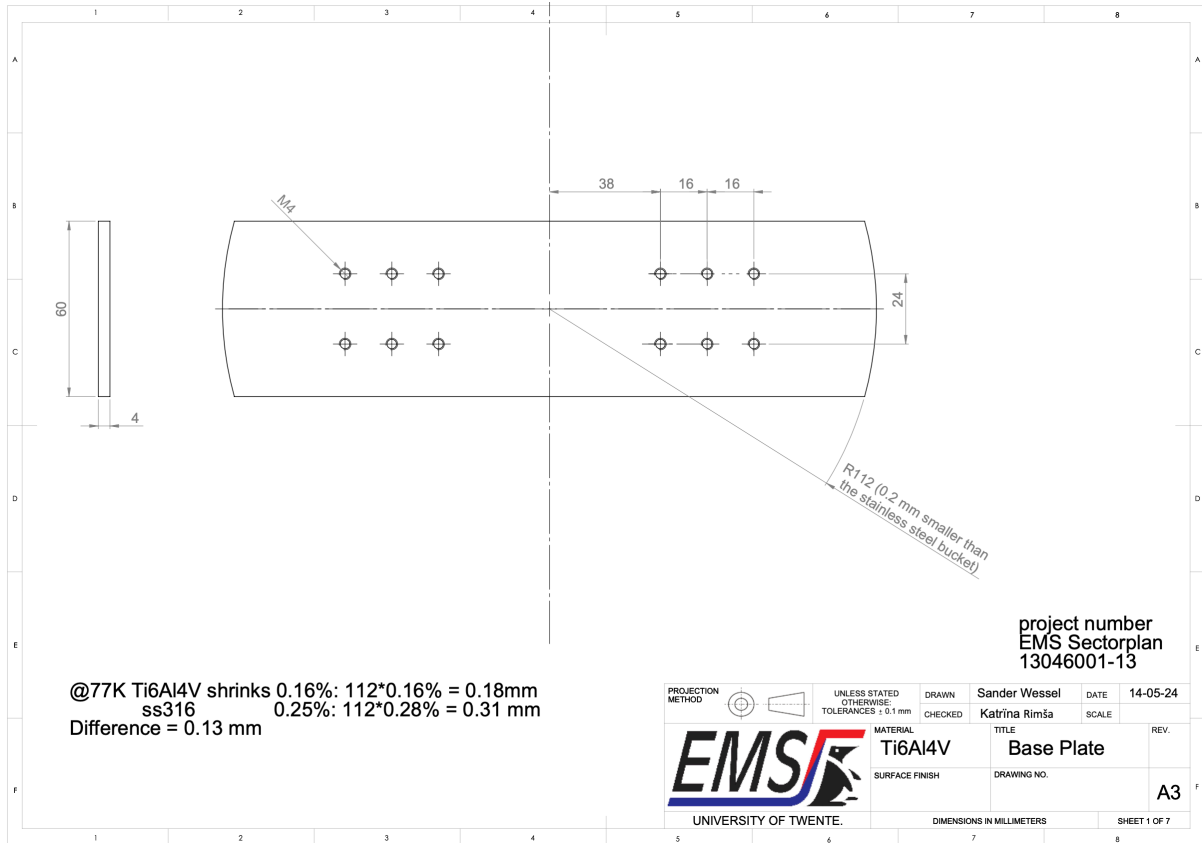
- [53] P. Gao, Y. Zhang, X. Wang, and Y. Zhou, "Interface properties and failures of REBCO coated conductor tapes: Research progress and challenges," *Superconductivity*, vol. 8, 2023. [Online]. Available: <https://www.sciencedirect.com/science/article/pii/S2772830723000339>
- [54] A.-J. Vialle, "Towards very high energy density insulated Rare-EarthBaCuO magnets," Ph.D. dissertation, Université Grenoble Alpes, 2022. [Online]. Available: <https://theses.fr/2022GRALT035>
- [55] T. Energy, "Fusion energy technology," 2024. [Online]. Available: <https://tokamakenergy.com/our-fusion-energy-and-hts-technology/fusion-energy-technology/>
- [56] Z. S. Hartwig, R. F. Vieira, B. N. Sorbom, R. A. Badcock, M. Bajko, W. K. Beck, B. Castaldo, C. L. Craighill, M. Davies, J. Estrada, V. Fry, T. Golfinopoulos, A. E. Hubbard, J. H. Irby, S. Kuznetsov, C. J. Lammi, P. C. Michael, T. Mouratidis, R. A. Murray, and A. T. Pfeiffer, "VIPER: an industrially scalable high-current high-temperature superconductor cable," *Superconductor Science and Technology*, vol. 33, no. 11, 2020.
- [57] P. Berkelman, "A novel coil configuration to extend the motion range of lorentz force magnetic levitation devices for haptic interaction," in *2007 IEEE/RSJ International Conference on Intelligent Robots and Systems*, 2007.
- [58] D. Uglietti, "A review of commercial high temperature superconducting materials for large magnets: from wires and tapes to cables and conductors," *Superconductor Science and Technology*, vol. 32, no. 5, 2019.
- [59] W. Zhou, R. Jia, J. Cao, and R. Liang, "Elastoplastic mechanical behavior of high-field magnet of REBCO high temperature superconducting composite tape under extreme environment," *Composite Structures*, vol. 329, 2024. [Online]. Available: <https://www.sciencedirect.com/science/article/pii/S0263822323011522>
- [60] H. Miyazaki, S. Iwai, T. Tosaka, K. Tasaki, and Y. Ishii, "Delamination strengths of different types of REBCO-coated conductors and method for reducing radial thermal stresses of impregnated REBCO pancake coils," *IEEE Transactions on Applied Superconductivity*, vol. 25, no. 3, 2015.
- [61] S. I. Bermudez, G. Sabbi, and A. V. Zlobin, "Accelerator Technology Magnets," 2022.
- [62] B. ten Haken, "Strain effects on the critical properties of high-field superconductors," Ph.D. dissertation, University of Twente, Enschede, The Netherlands, 1994.
- [63] Fujifilm, "Prescale," 2024. [Online]. Available: <https://www.fujifilm.com/de/de/business/inspection/measurement-film/prescale>
- [64] I. A. Shahid, "Sandpaper defect detection," Master's Thesis, Åbo Akademi University, 2021. [Online]. Available: [https://www.doria.fi/bitstream/handle/10024/181261/shahid\\_imran.pdf?sequence=3&isAllowed=y](https://www.doria.fi/bitstream/handle/10024/181261/shahid_imran.pdf?sequence=3&isAllowed=y)
- [65] K. Artoos, D. Clair, A. Poncet, F. Savary, and R. Veness, "The measurement of friction coefficient down to 1.8 K for LHC magnets," in *Fifteenth International Cryogenic Engineering Conference ICEC 15*, Genova, Italy, June 1994. [Online]. Available: <https://cds.cern.ch/record/1019470/files/CM-P00062282.pdf>

- [66] D. Aized, J. W. Haddad, C. H. Joshi, L. F. Goodrich, and A. N. Srivastava, "Comparing the accuracy of critical-current measurements using the voltage-current simulator," *IEEE Transactions on Magnetics*, vol. 30, no. 4, 1994.
- [67] Datona, "Werkplaatspers 10 ton online kopen," 2024. [Online]. Available: <https://www.datona.nl/werkplaatspers-10-ton/>
- [68] S. Lee, V. Petrykin, A. Molodyk, S. Samoilenkov, A. Kaul, A. Vavilov, V. Vysotsky, and S. Fetisov, "Development and production of second generation high T<sub>c</sub> superconducting tapes at SuperOx and first tests of model cables," *Superconductor Science and Technology*, vol. 27, no. 4, mar 2014.
- [69] X. Wang, U. P. Trociewitz, and J. Schwartz, "Critical current degradation of short YBa<sub>2</sub>Cu<sub>3</sub>O<sub>7</sub> coated conductor due to an unprotected quench," *Superconductor Science and Technology*, vol. 24, no. 3, December 2010.
- [70] J. P. (2022, March 26) Uncertainties in physics. The Tutor Team. [Online]. Available: <https://www.thetutorteam.com/science/uncertainties-in-physics/>
- [71] X. Wang, A. B. Yahia, E. Bosque, P. Ferracin, S. Gourlay, R. Gupta, H. Higley, V. Kashikhin, M. Kumar, V. Lombardo *et al.*, "REBCO—a silver bullet for our next high-field magnet and collider budget?" 2022.
- [72] A. Negri della Torre, "Regulating compact nuclear fusion," *SSRN Electronic Journal*, 2018.

# Appendix

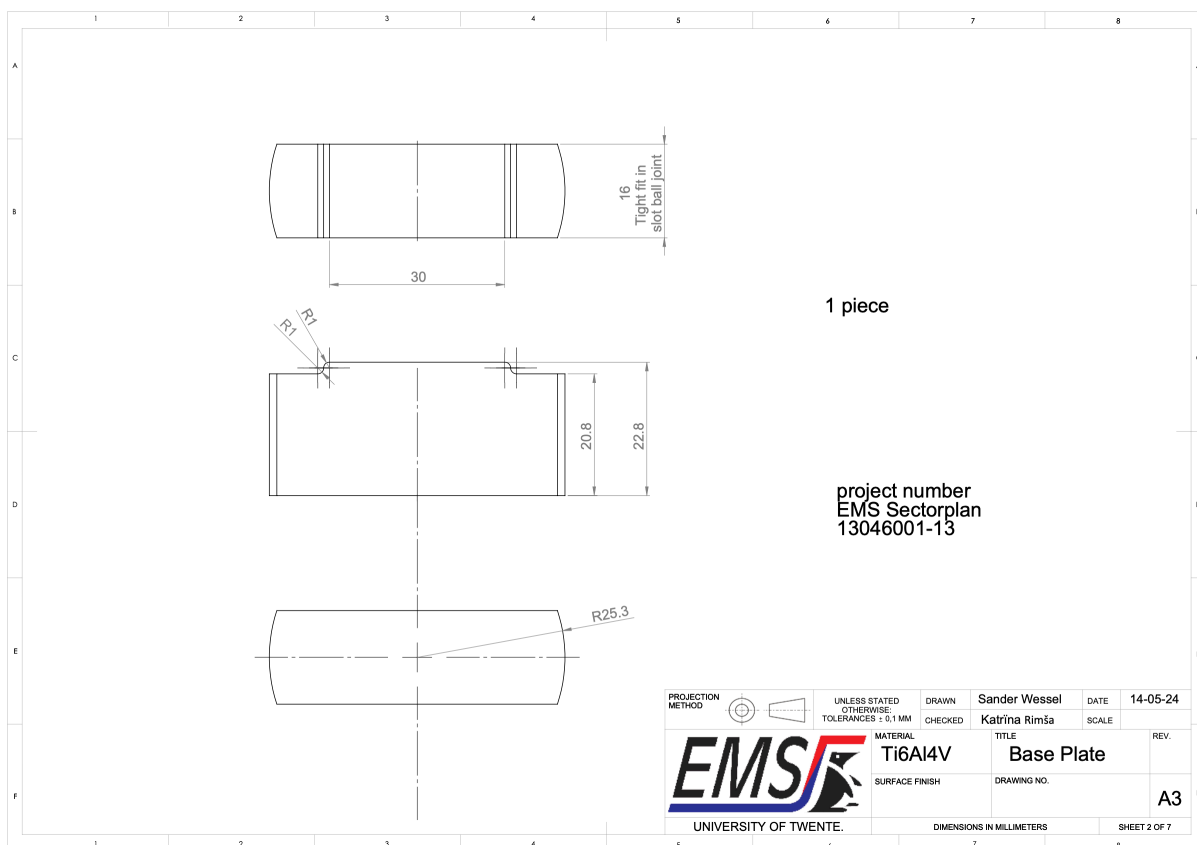
## Technical Drawings for the Rintje Ritsma Press Assembly Items

### Titanium base plate

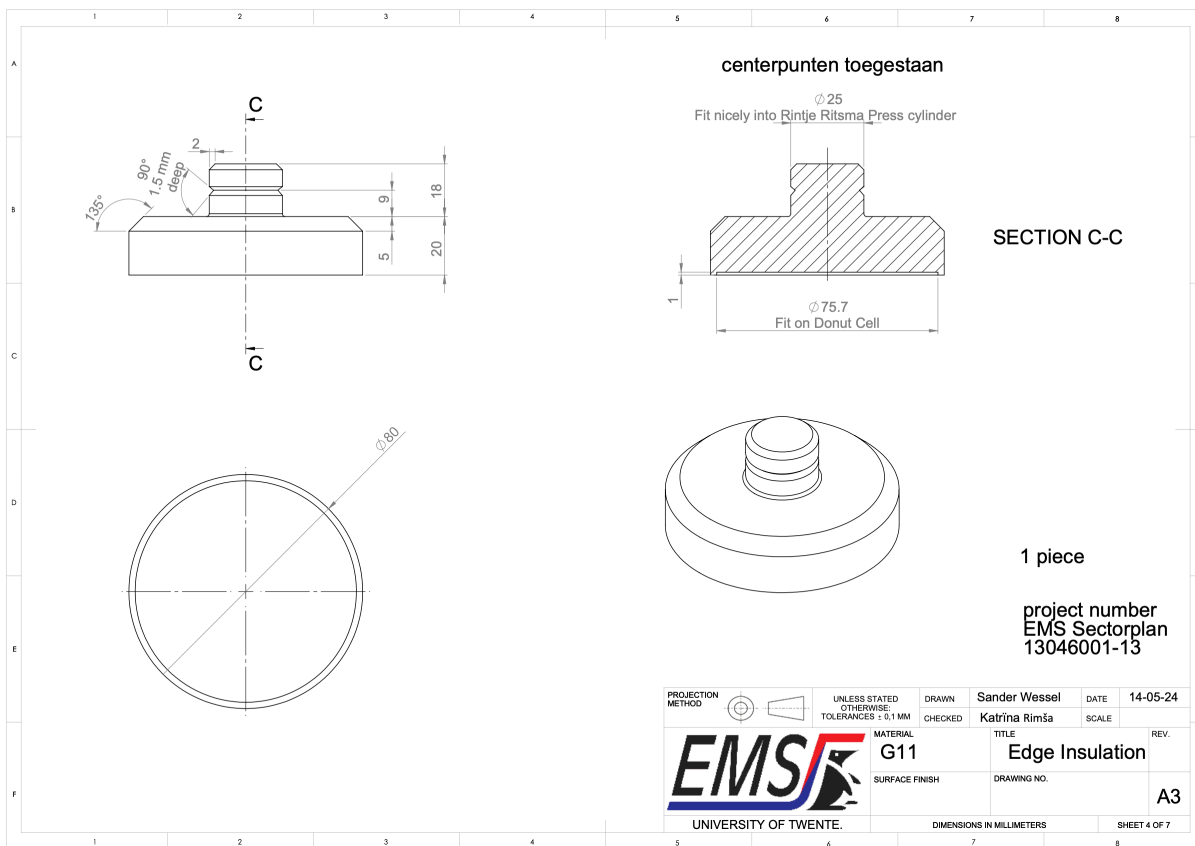




### Titanium pushing block




**Brass adaptor**

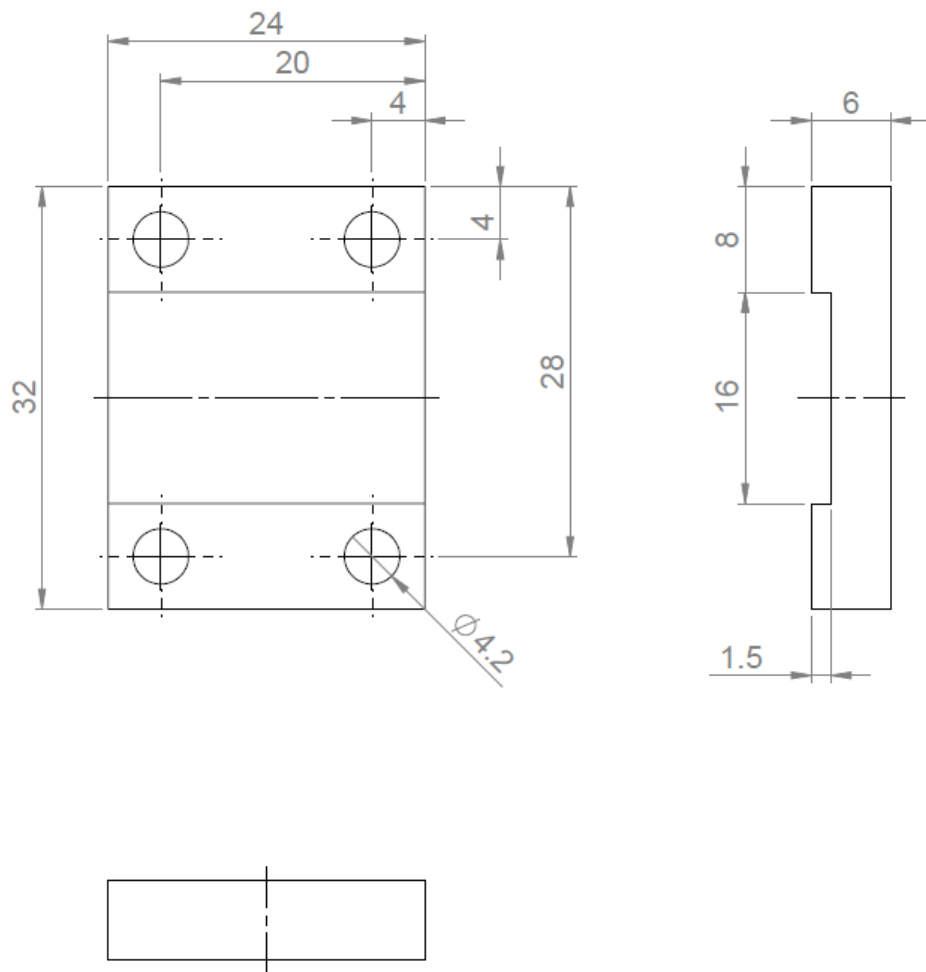


SECTION C-C

1 piece

project number  
EMS Sectorplan  
13046001-13

PROJECTION METHOD	UNLESS STATED OTHERWISE: TOLERANCES : 0.1 MM	DRAWN	Sander Wessel	DATE	14-05-24
		CHECKED	Katrina Rimša	SCALE	
 UNIVERSITY OF TWENTE.		MATERIAL	TITLE		
		G11	Edge Insulation		
		SURFACE FINISH	DRAWING NO.		REV.
					A3
DIMENSIONS IN MILLIMETERS					SHEET 4 OF 7

**Copper blocks**

### G11 voltage taps

ITEM NO.	PART NUMBER	QTY.
1	V-tap G11 plate	1
2	Voltage top small G11	1
3	Washer ISO 7089 - 4	2
4	ISO - 4032 - M4 - W - N	2
5	V-tap Copper foil	1
6	Voltage tap indium foil	1
7	Voltage tap wire	1
8	Voltage tap M4 thread	2

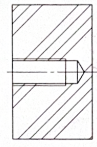
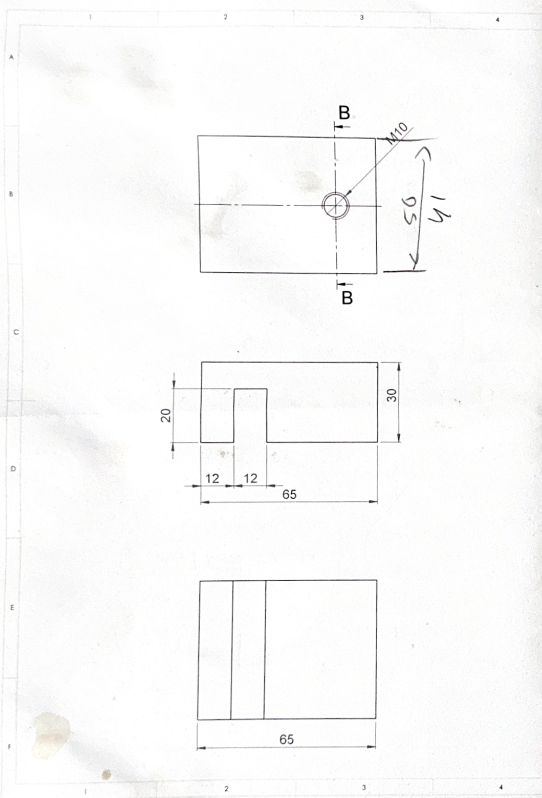
**Glue part 2 on part 1**  
**next glue copper foil (0.1mm or so) on part 2**  
**Voltage tap wire solder on the Copper foil**  
**Indium foil after placing the tape on the holder**

**project number**  
**EMS Sectorplan**  
**13046001-13**

PROJECTION METHOD	UNLESS STATED OTHERWISE TOLERANCES ± 0.5 MM	DRAWN	Sander Wessel	DATE	14-05-24
		CHECKED	Katrina Rimša	SCALE	
		MATERIAL	TITLE		REV.
		G11	Voltage tap		
		SURFACE FINISH	DRAWING NO.		A3
UNIVERSITY OF TWENTE.					SHEET 6 OF 7

DIMENSIONS IN MILLIMETERS

# G11 edge blocks



SECTION B-B  
SCALE 1 : 1

2 pieces

project number  
EMS Sectorplan  
13046001-13

PROJECTION METHOD		UNLESS STATED OTHERWISE TOLERANCES : 0.5 MM	DRAWN	Sander Wessel	DATE	14-05-24
			CHECKED	Katrina Rimša	SCALE	
		MATERIAL	TITLE		REV.	
UNIVERSITY OF TWENTE		G11	Edge Insulation			
		SURFACE FINISH	DRAWING NO.		A3	
DIMENSIONS IN MILLIMETERS			SHEET 3 OF 8			